Supporting Information

for

Synthesis, spectroscopic characterization and thermogravimetric analysis of two series of substituted (metallo)tetraphenylporphyrins

Rasha K. Al-Shewiki[1], Carola Mende[1], Roy Buschbeck[1], Pablo F. Siles[2,3], Oliver G. Schmidt[2,3], Tobias Rüffer*[1] and Heinrich Lang[1]

Address: [1]Inorganic Chemistry, Institute of Chemistry, Faculty of Natural Sciences, TU Chemnitz, 09107 Chemnitz, Germany; [2]Material Systems for Nanoelectronics, TU Chemnitz, 09107 Chemnitz, Germany and [3]Institute for Integrative Nanosciences, IFW Dresden, Helmholtzstrasse 20, 01069 Dresden, Germany

Email: Tobias Rüffer* - tobias.rueffer@chemie.tu-chemnitz.de

* Corresponding author

Additional experimental data

Table of contents

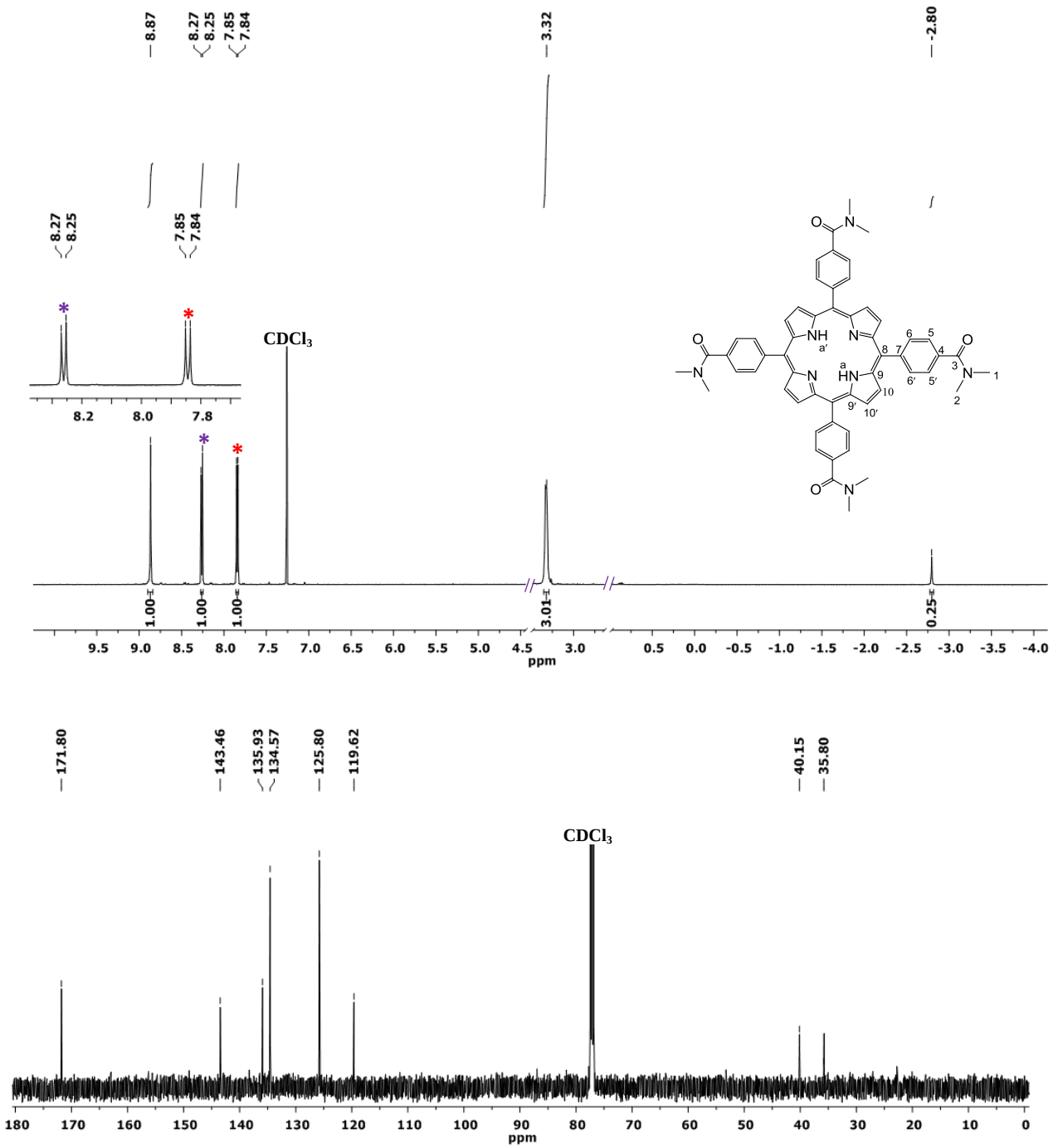

Figure S1: ^{1}H (above) and ^{13}C{^{1}H} NMR spectra (below) of **2**.

According to Jones and Wilkins [S1] for the -NMe_2 groups two ^{13}C NMR chemical shifts are observed. According to Manke et al. [S2] the ^{13}C NMR resonances of the pyrrole carbon atoms $C^{9,9'}$ and $C^{10,10'}$ are not observable.

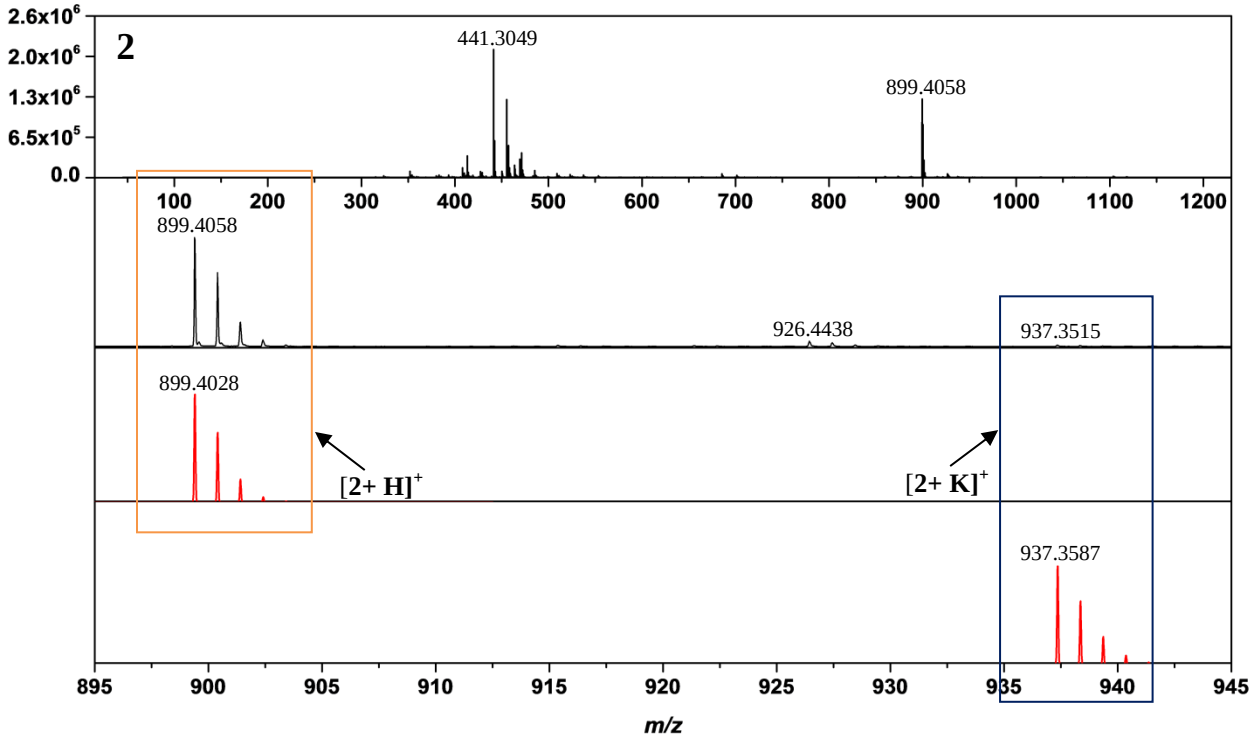

Figure S2: ESI-MS spectrum of **2**.

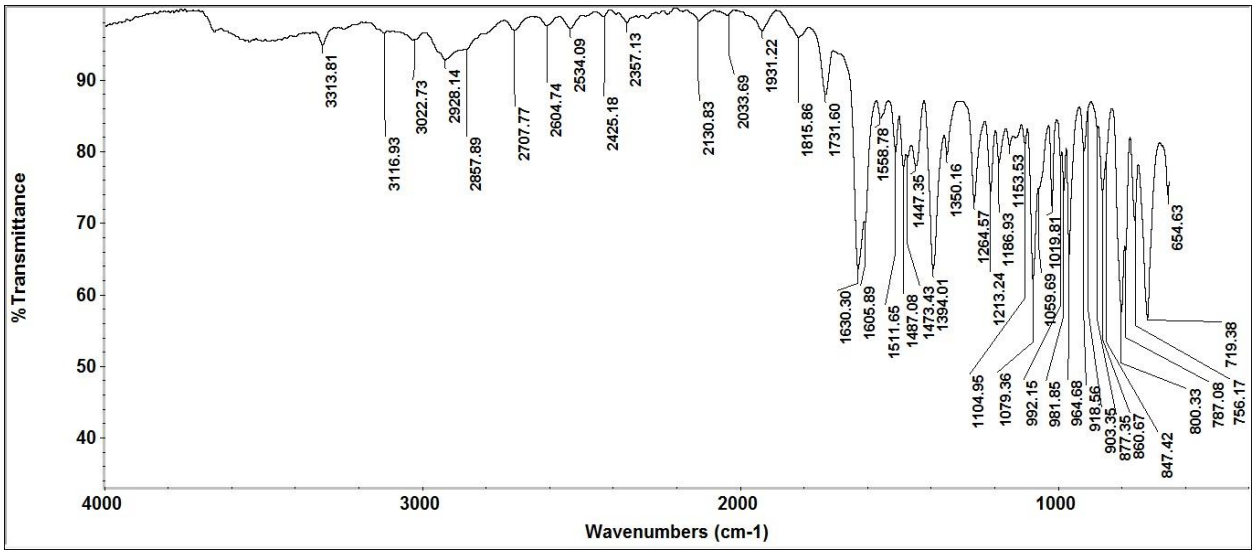

Figure S3a: IR spectrum (ATR-IR) of **2**.

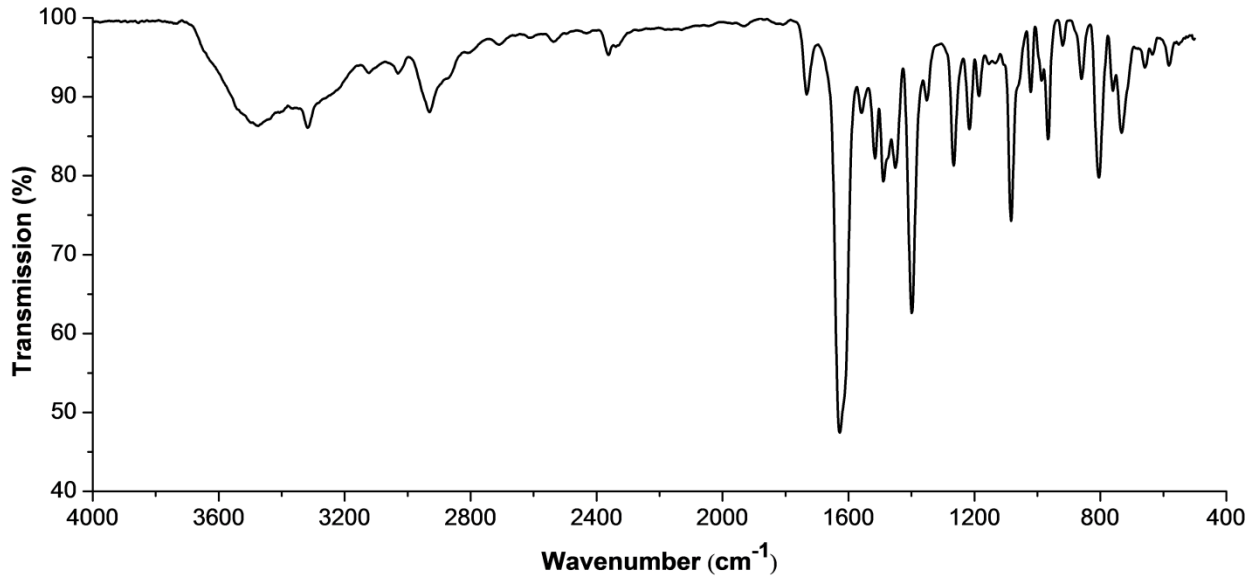

Figure S3b: IR spectrum (KBr) of **2**.

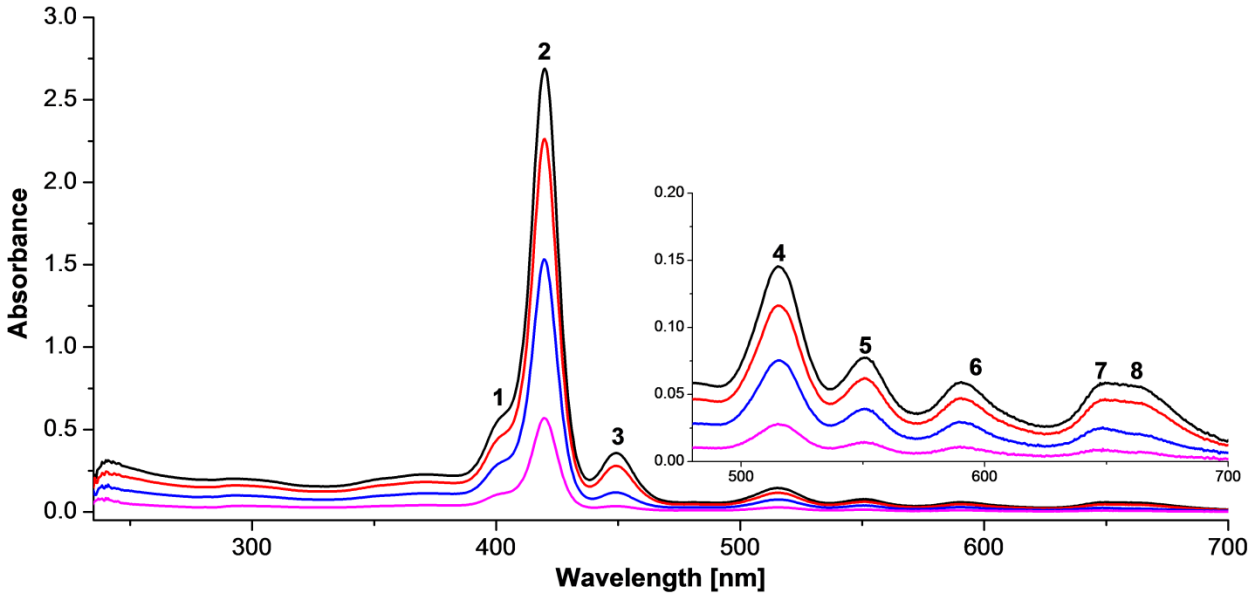

Figure S4: UV–vis spectrum of **2** in $CHCl_3$ at different concentrations.

Table S1: UV–vis data (λ_{max} [nm] log (ε [$L \cdot mol^{-1} \cdot cm^{-1}$])) of **2** at different concentrations.

	Absorption λ_{max} [nm] log (ε [$L \cdot mol^{-1} \cdot cm^{-1}$])							
	1	**2**	**3**	**4**	**5**	**6**	**7**	**8**
C_1 = 8.620·10^{-6} mol/L	400.8 (4.81)	419.8 (5.49)	449.3 (4.63)	515.6 (4.23)	550.6 (3.951)	590.8 (3.84)	647 (3.83)	665.5 (3.81)
C_2 = 5.172·10^{-6} mol/L	400.8 (4.93)	419.8 (5.64)	449.3 (4.74)	515.6 (4.35)	550.6 (4.08)	590.8 (3.96)	647 (3.93)	665.5 (3.93)
C_3 = 1.724·10^{-6} mol/L	400.8 (5.24)	419.8 (5.95)	449.3 (4.83)	515.6 (4.64)	550.6 (4.36)	590.8 (3.24)	647 (4.17)	666.3 (4.07)
C_4 = 3.448·10^{-6} mol/L	400.8 (4.49)	419.8 (5.22)	449.3 (4.05)	515.6 (3.90)	550.6 (3.64)	590.8 (3.51)	647 (3.41)	666.3 (3.41)

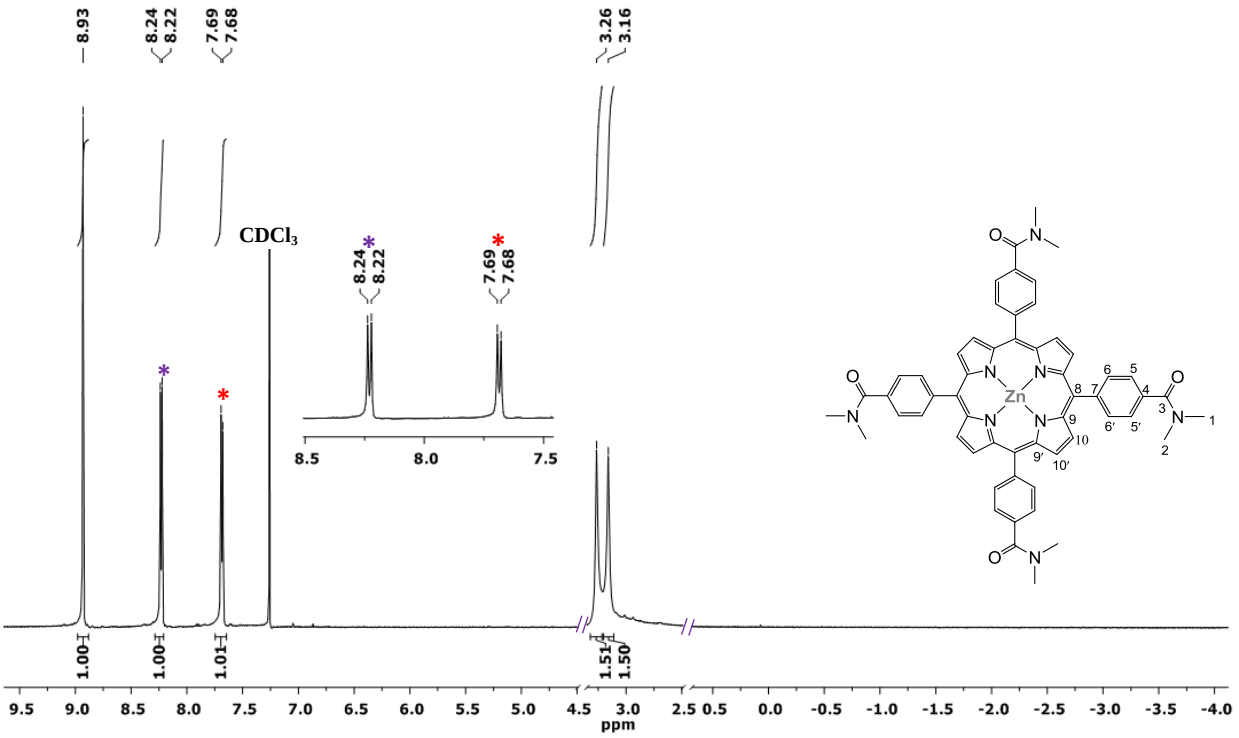

Figure S5: ^{1}H NMR spectrum of **2a**.

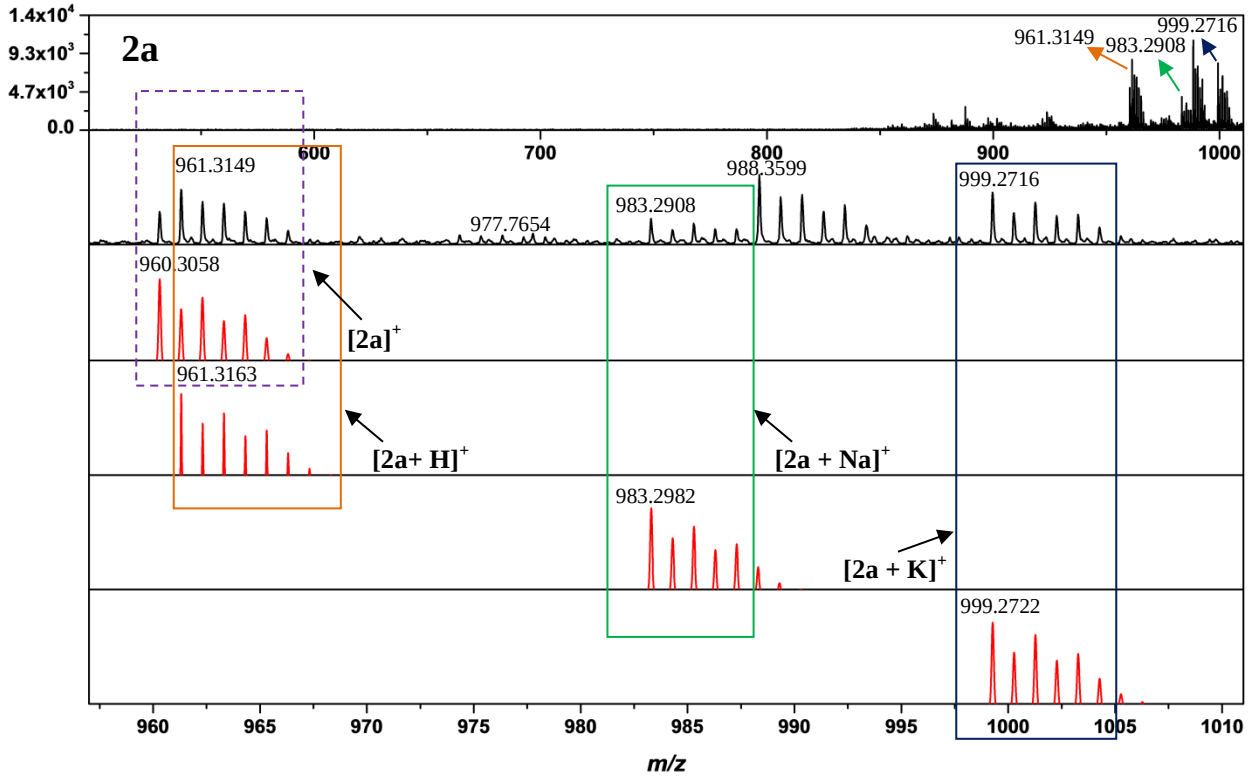

Figure S6: ESI-MS spectrum of **2a** (Black: Measured. Red: Calculated).

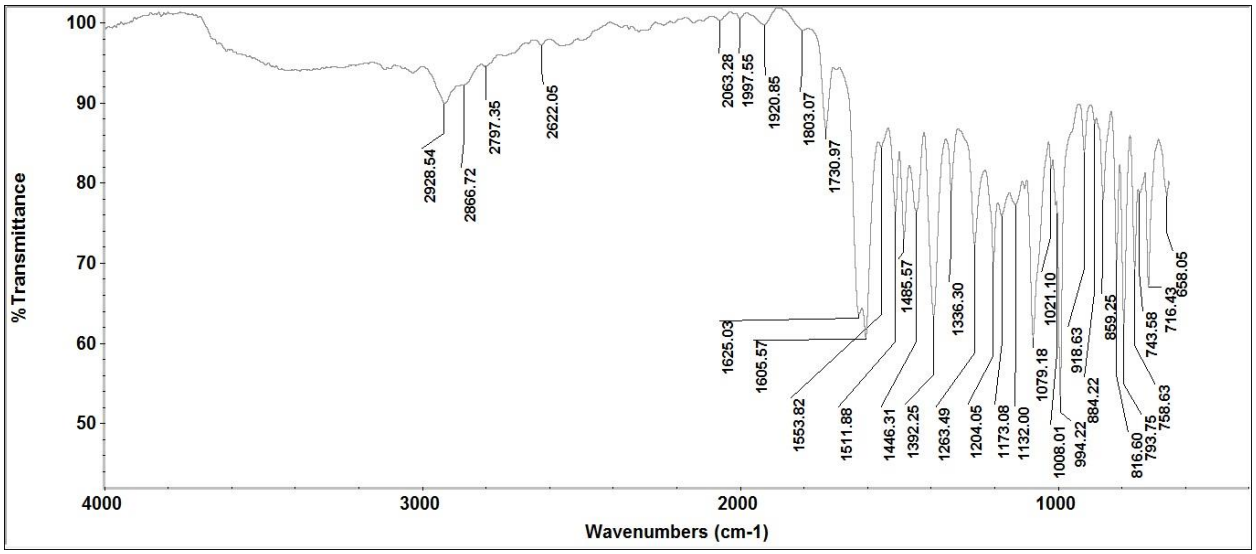

Figure S7a: IR spectrum (ATR-IR) of **2a**.

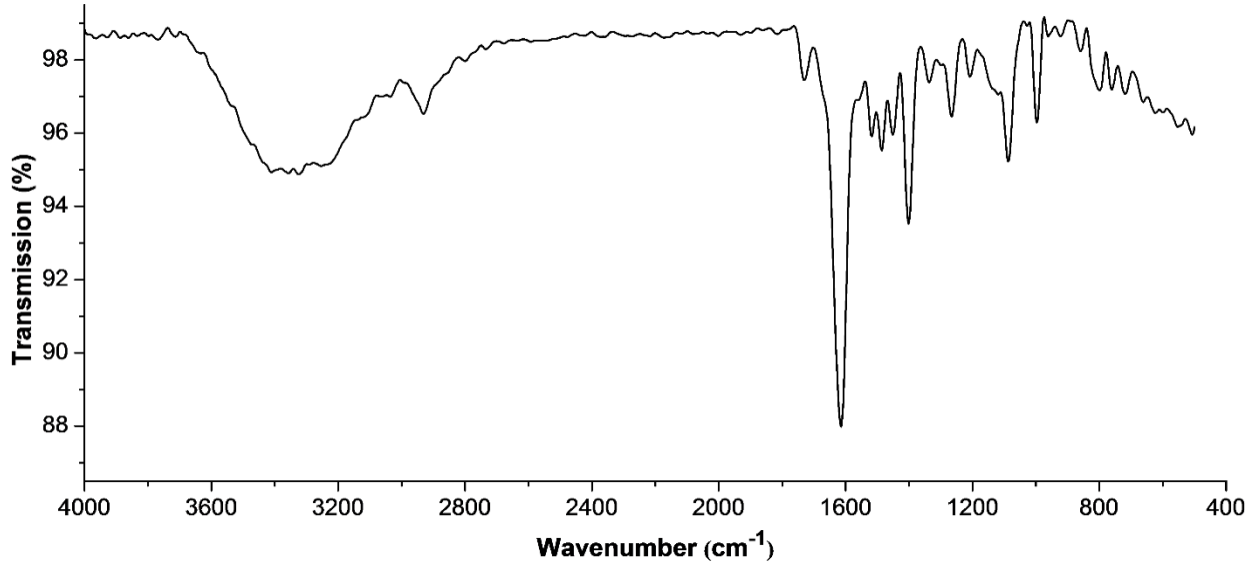

Figure S7b: IR spectrum (KBr) of **2a**.

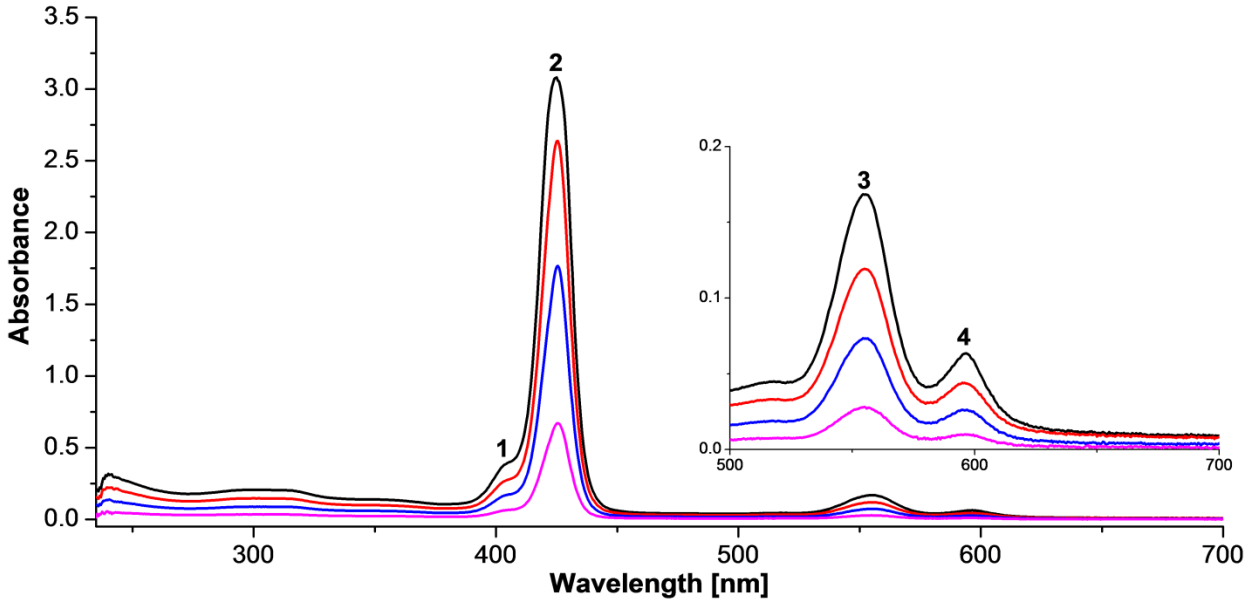

Figure S8: UV–vis spectrum of **2a** in $CHCl_3$ at different concentrations.

Table S2: UV–vis data (λ_{max} [nm] log (ε [L·mol^{-1}·cm^{-1}])) of **2a** at different concentrations.

	Absorption λ_{max} [nm] log (ε [L·mol^{-1}·cm^{-1}])			
	1	**2**	**3**	**4**
C_1 = 1.127·10^{-5} mol/L	403.4 (4.54)	425.1 (5.44)	555.1 (4.18)	596.3 (3.75)
C_2 = 8.053·10^{-6} mol/L	403.4 (4.54)	425.1 (5.51)	555.1 (4.17)	596.3 (3.74)
C_3 = 4.832·10^{-6} mol/L	403.4 (4.55)	425.6 (5.55)	555.1 (4.19)	596.3 (3.73)
C_4 = 1.611·10^{-6} mol/L	403.4 (4.60)	425.6 (5.62)	555.1 (4.22)	596.3 (3.77)

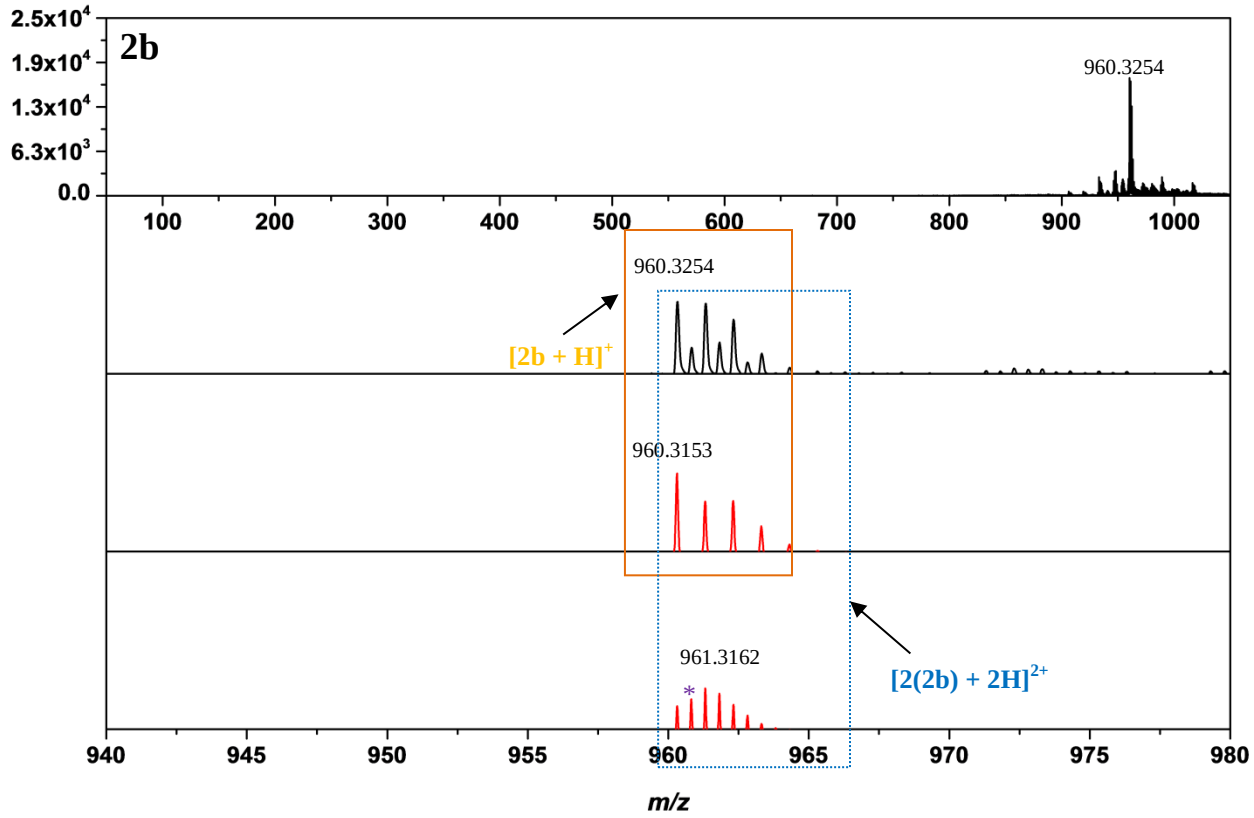

Figure S9: ESI-MS spectrum of **2b** (Black: Measured. Red: Calculated).

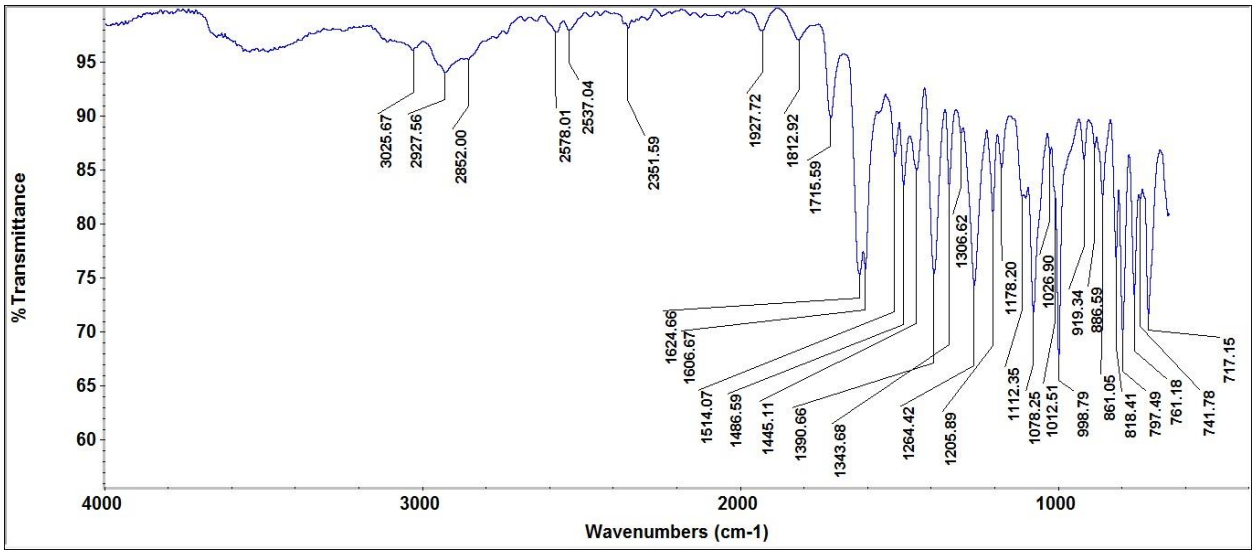

Figure S10a: IR spectrum (ATR-IR) of **2b**.

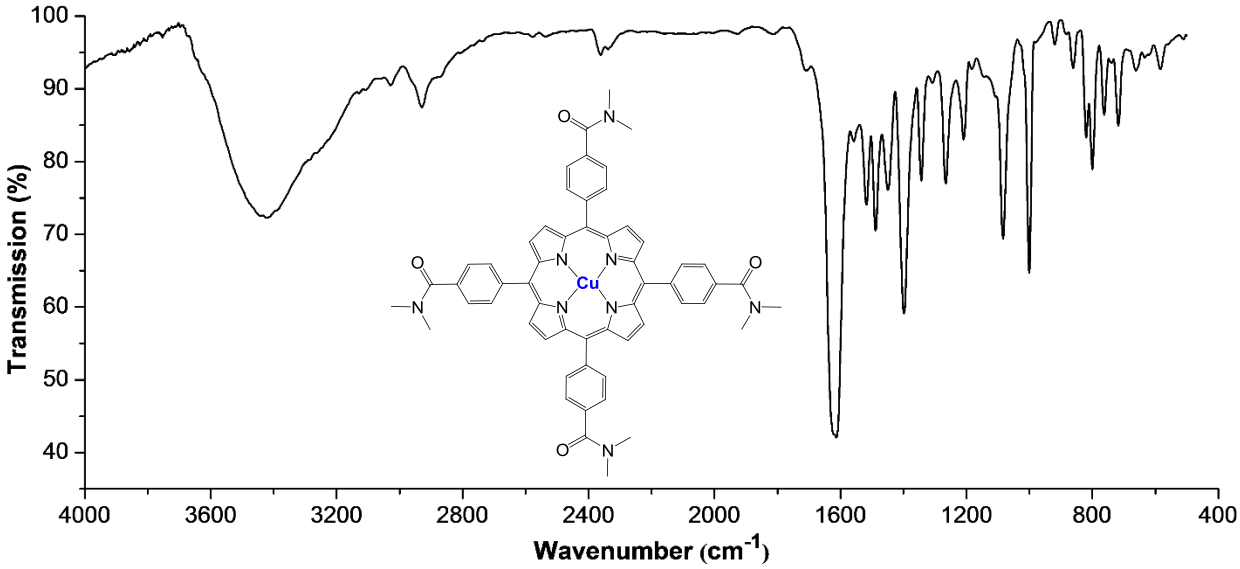

Figure S10b: IR spectrum (KBr) of **2b**.

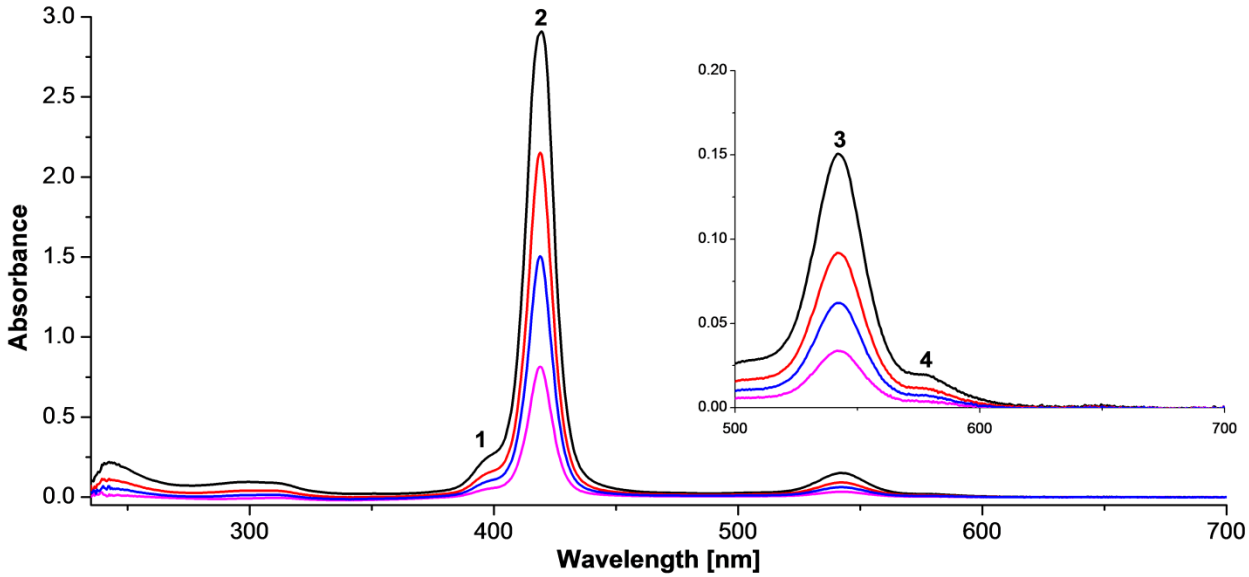

Figure S11: UV–vis spectrum of **2b** in $CHCl_3$ at different concentrations.

Table S3: UV–vis data (λ_{max} [nm] log (ε [L·mol^{-1}·cm^{-1}])) of **2b** at different concentrations.

	Absorption λ_{max} [nm] log (ε [L·mol^{-1}·cm^{-1}])			
	1	**2**	**3**	**4**
C_1 = 8.328·10^{-6} mol/L	396 (4.48)	419.2 (5.54)	542.7 (4.26)	578.4 (3.38)
C_2 = 4.997·10^{-6} mol/L	396 (4.47)	419.2 (5.63)	542.7 (4.27)	578.4 (3.40)
C_3 = 3.331·10^{-6} mol/L	396 (4.44)	419.2 (5.65)	542.7 (4.28)	578.4 (3.39)
C_4 = 1.661·10^{-6} mol/L	396 (4.45)	419.2 (5.68)	542.7 (4.31)	578.4 (3.37)

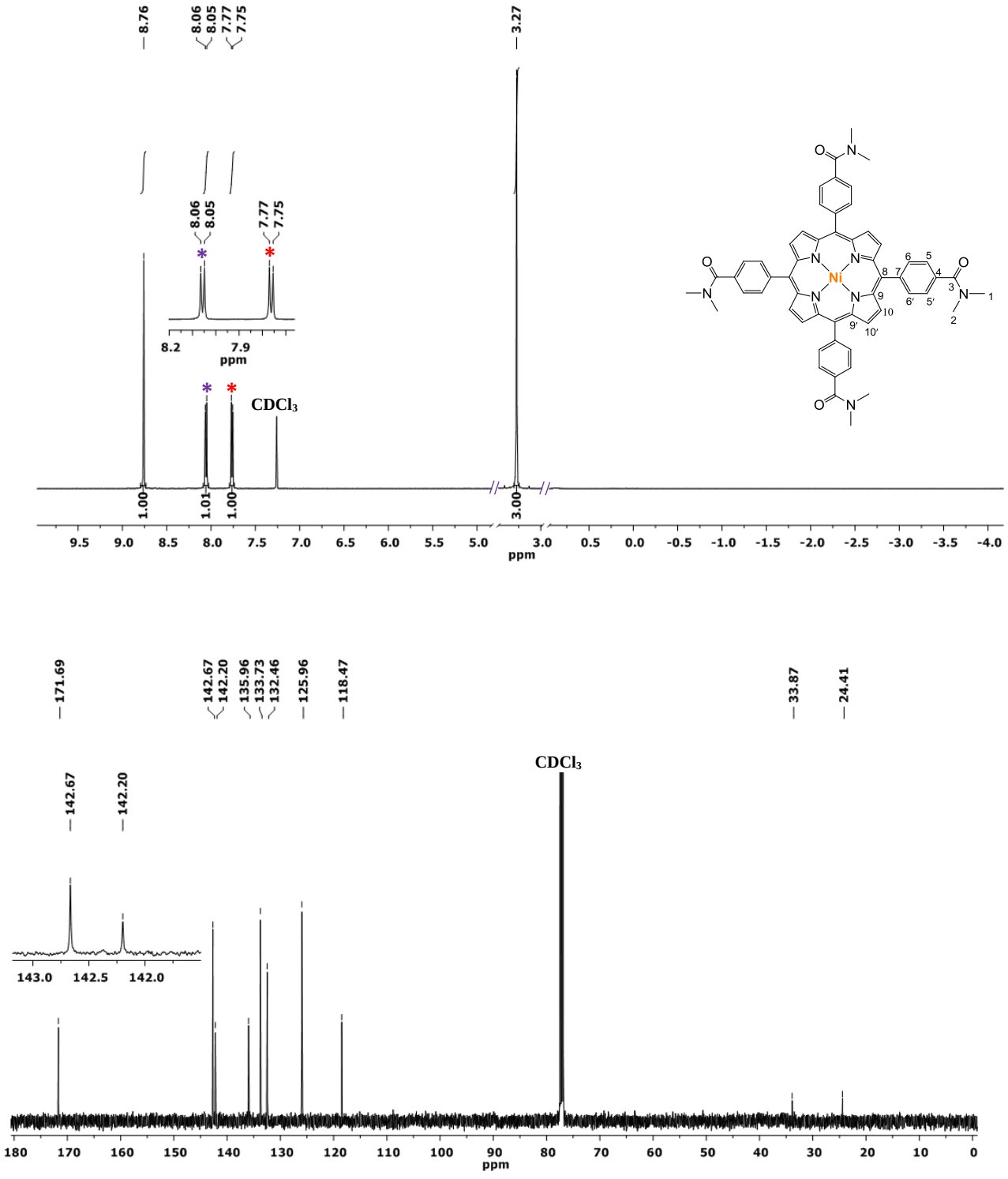

Figure S12: ^{1}H (above) and ^{13}C{^{1}H} NMR spectra (below) of **2c**.

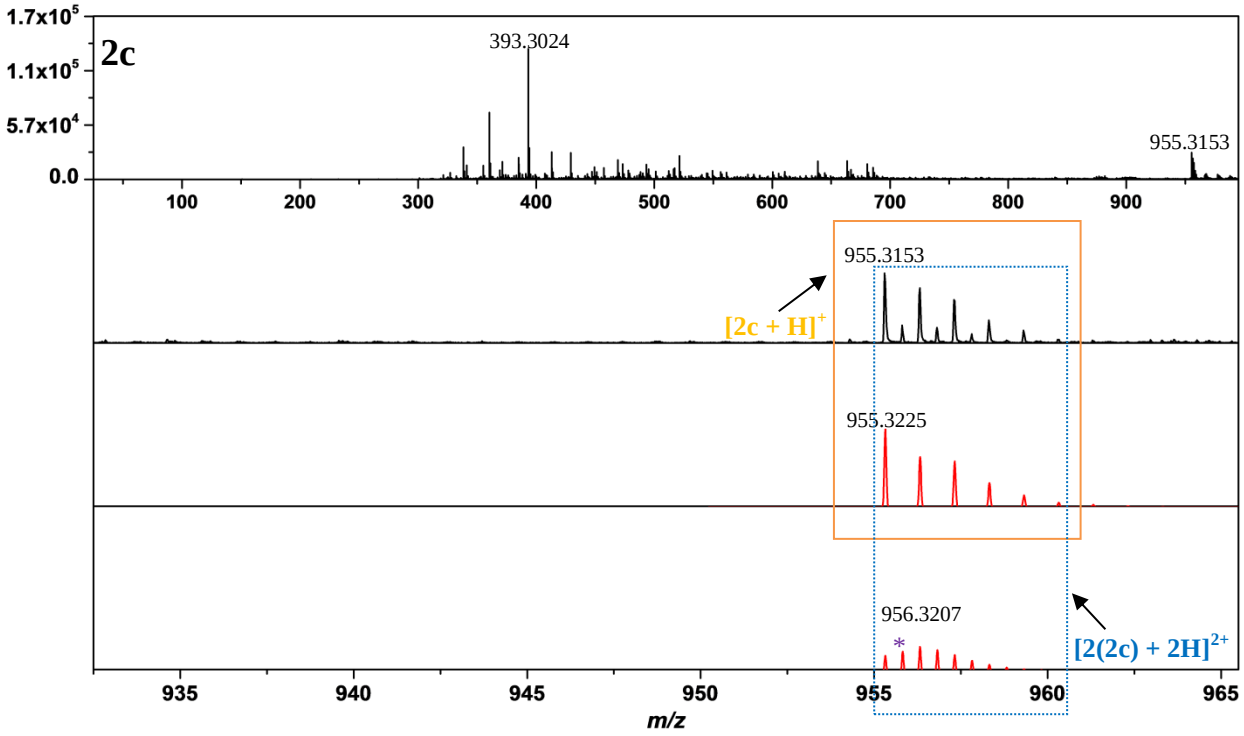

Figure S13: ESI-MS spectrum of **2c** (Black: Measured. Red: Calculated).

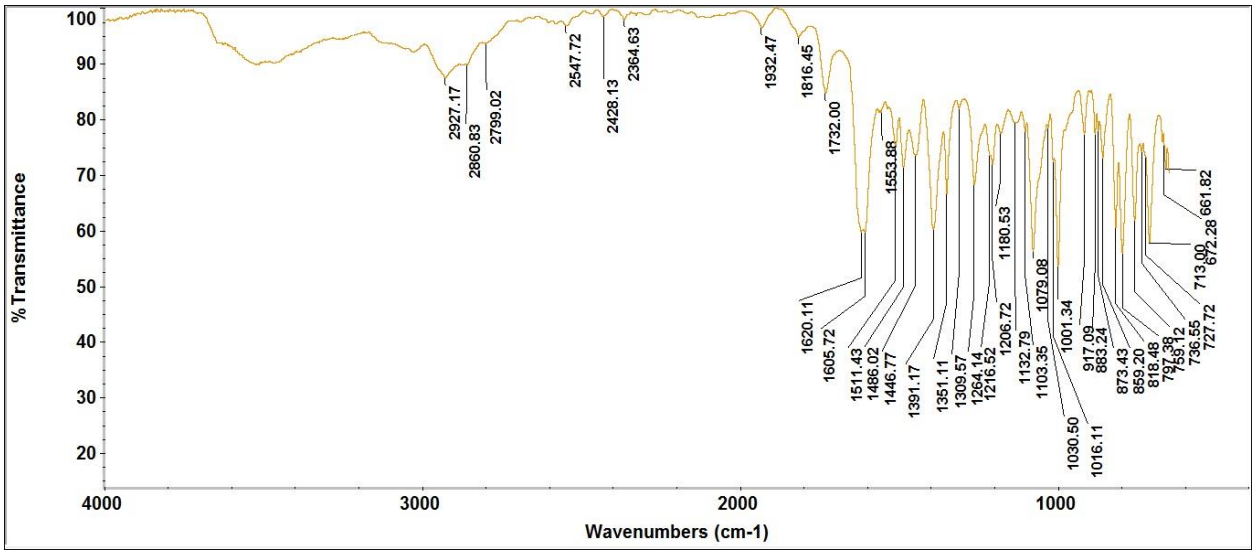

Figure S14a: IR spectrum (ATR-IR) of **2c**.

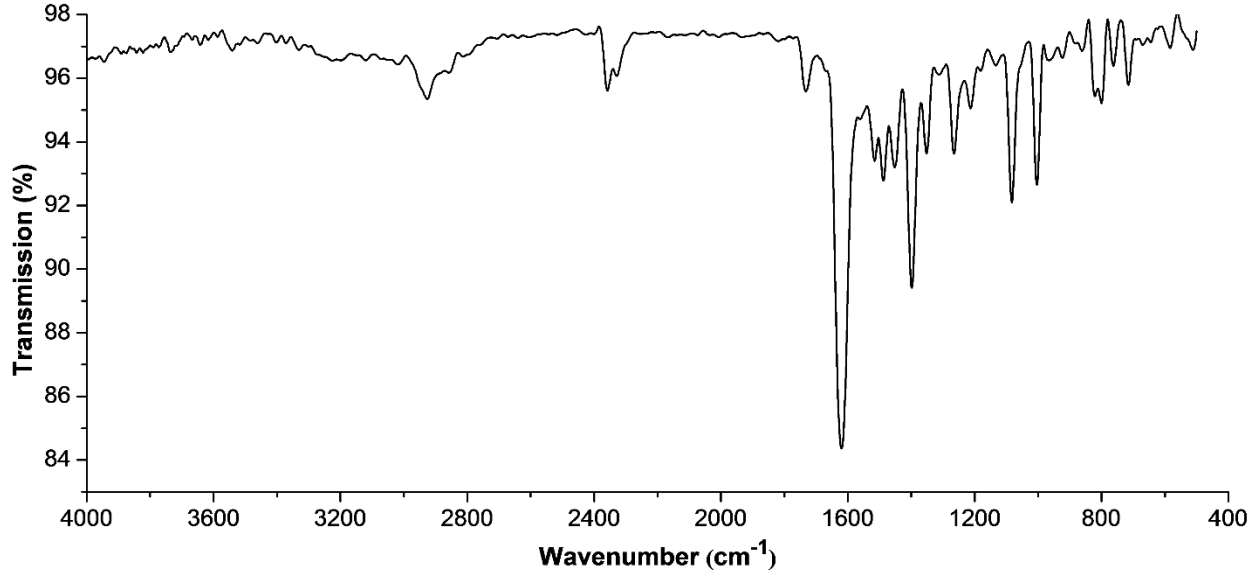

Figure S14b: IR spectrum (KBr) of **2c**.

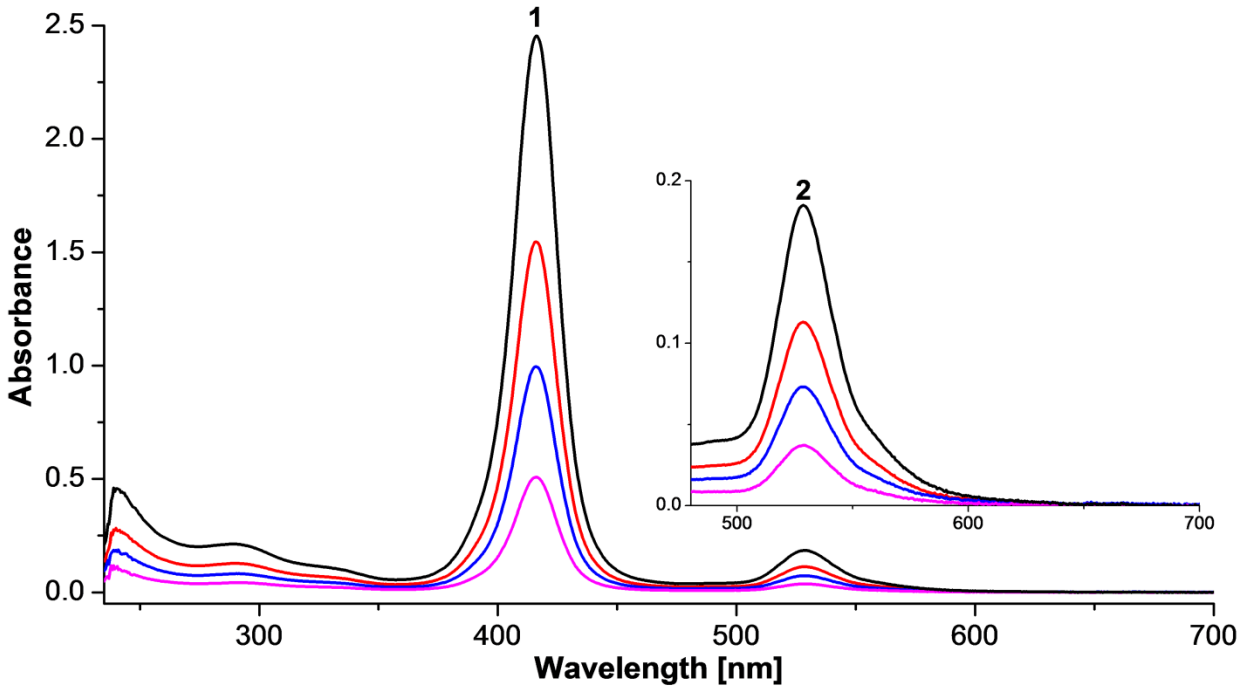

Figure S15: UV–vis spectrum of **2c** in $CHCl_3$ at different concentrations.

Table S4: UV–vis data (λ_{max} [nm] log (ε [L·mol $^{-1}$·cm^{-1}])) of **2c** at different concentrations.

	Absorption λ_{max} [nm] log (ε [L·mol^{-1}·cm^{-1}])	
	1	**2**
C_1 = **1.282·10^{-5} mol/L**	416.2 (5.28)	528.2 (4.16)
C_2 = **7.691·10^{-6} mol/L**	416.2 (5.30)	528.2 (4.17)
C_3 = **5.127·10^{-6} mol/L**	416.2 (5.29)	528.2 (4.16)
C_4 = **2.564·10^{-6} mol/L**	416.2 (5.30)	528.2 (4.16)

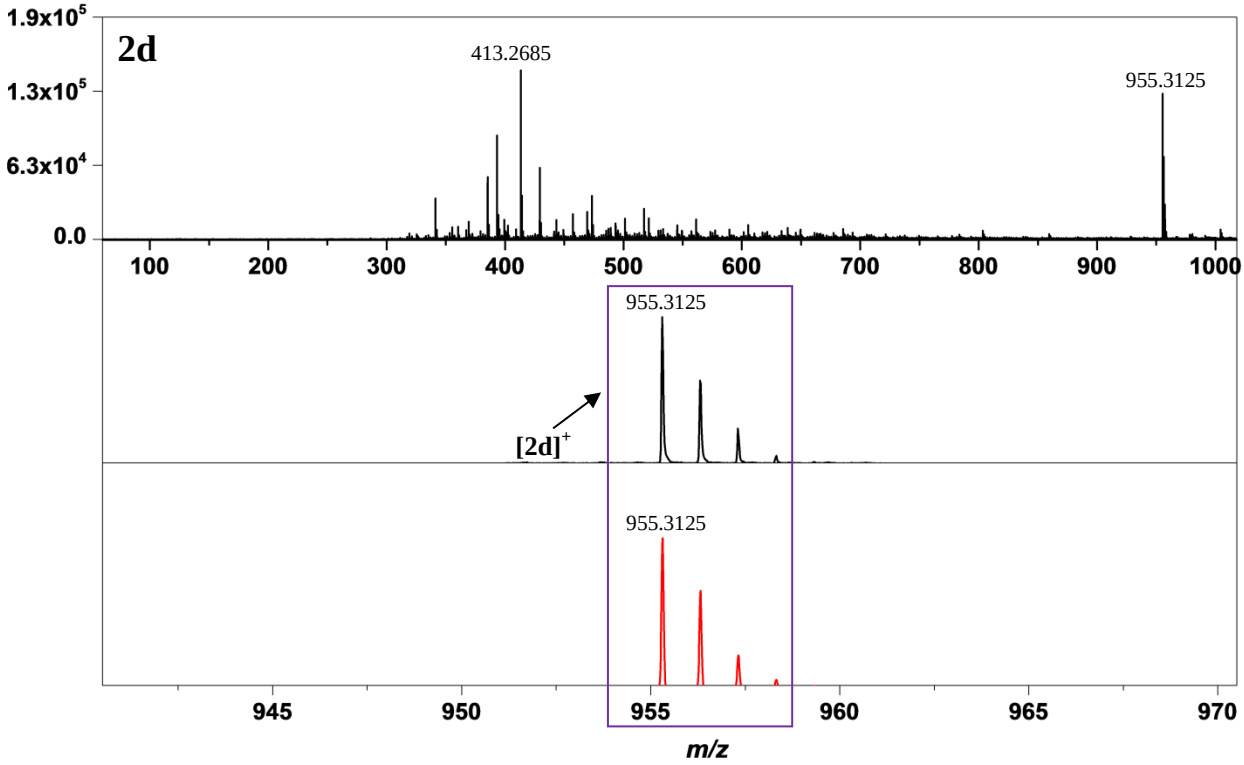

Figure S16: ESI-MS spectrum of **2d** (Black: Measured. Red: Calculated).

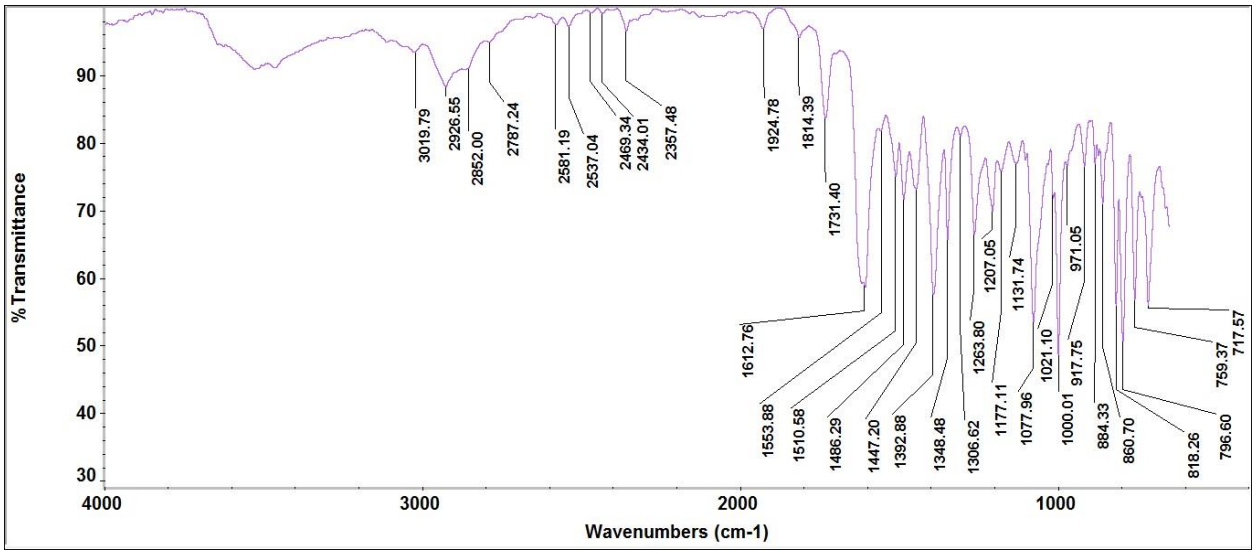

Figure S17a: IR spectrum (ATR-IR) of **2d**.

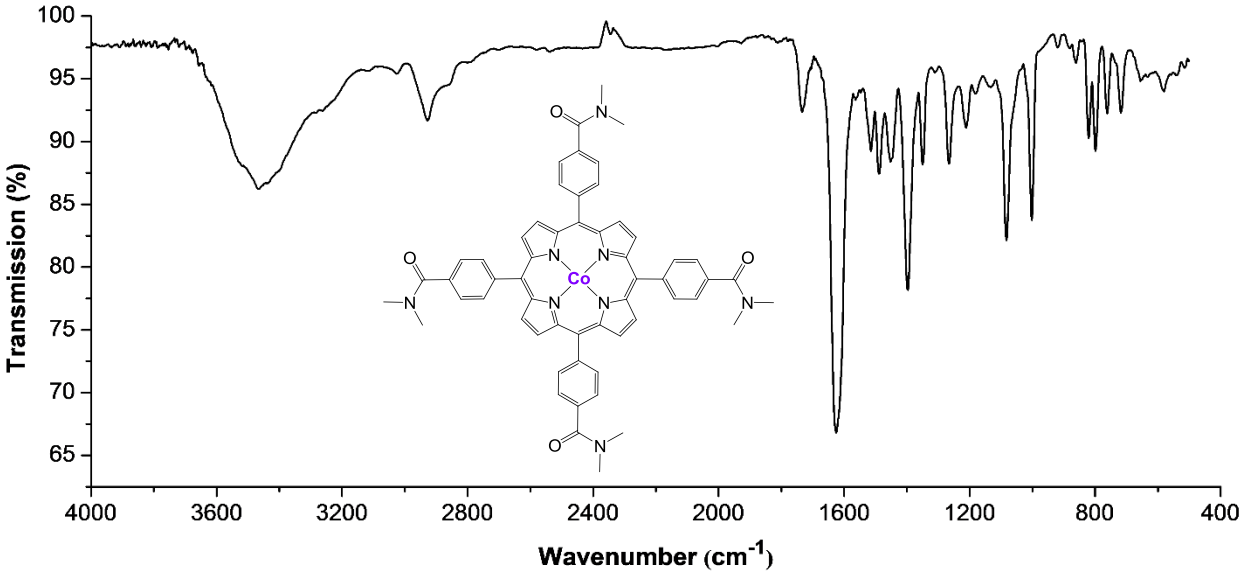

Figure S17b: IR spectrum (KBr) of **2d**.

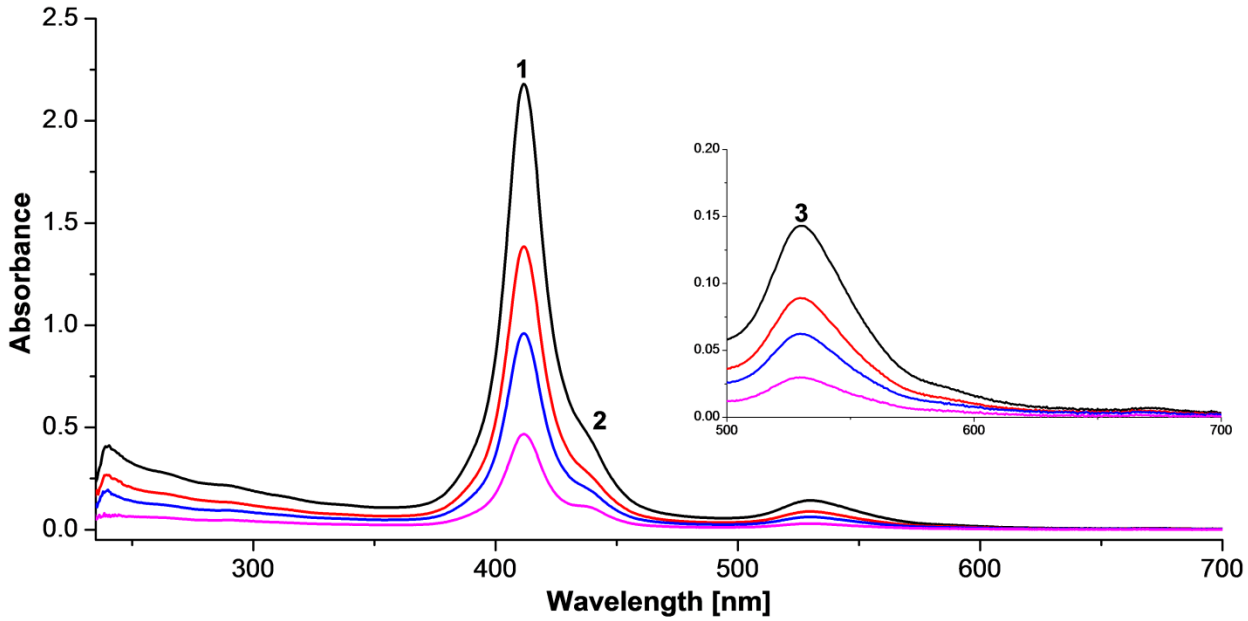

Figure S18: UV–vis spectrum of **2d** in $CHCl_3$ at different concentrations.

Table S5: UV–vis data (λ_{max} [nm] log (ε [$L \cdot mol^{-1} \cdot cm^{-1}$])) of **2d** at different concentrations.

	Absorption λ_{max} [nm] log (ε [$L \cdot mol^{-1} \cdot cm^{-1}$])		
	1	**2**	**3**
C_1 = **$1.172 \cdot 10^{-5}$ mol/L**	411.9 (5.26)	442.3 (4.50)	530 (4.09)
C_2 = **$8.368 \cdot 10^{-6}$ mol/L**	411.9 (5.24)	442.3 (4.44)	530 (4.03)
C_3 = **$5.021 \cdot 10^{-6}$ mol/L**	411.9 (5.28)	442.3 (4.53)	530 (4.10)
C_4 = **$1.674 \cdot 10^{-6}$ mol/L**	411.9 (5.45)	441.6 (4.83)	530 (4.26)

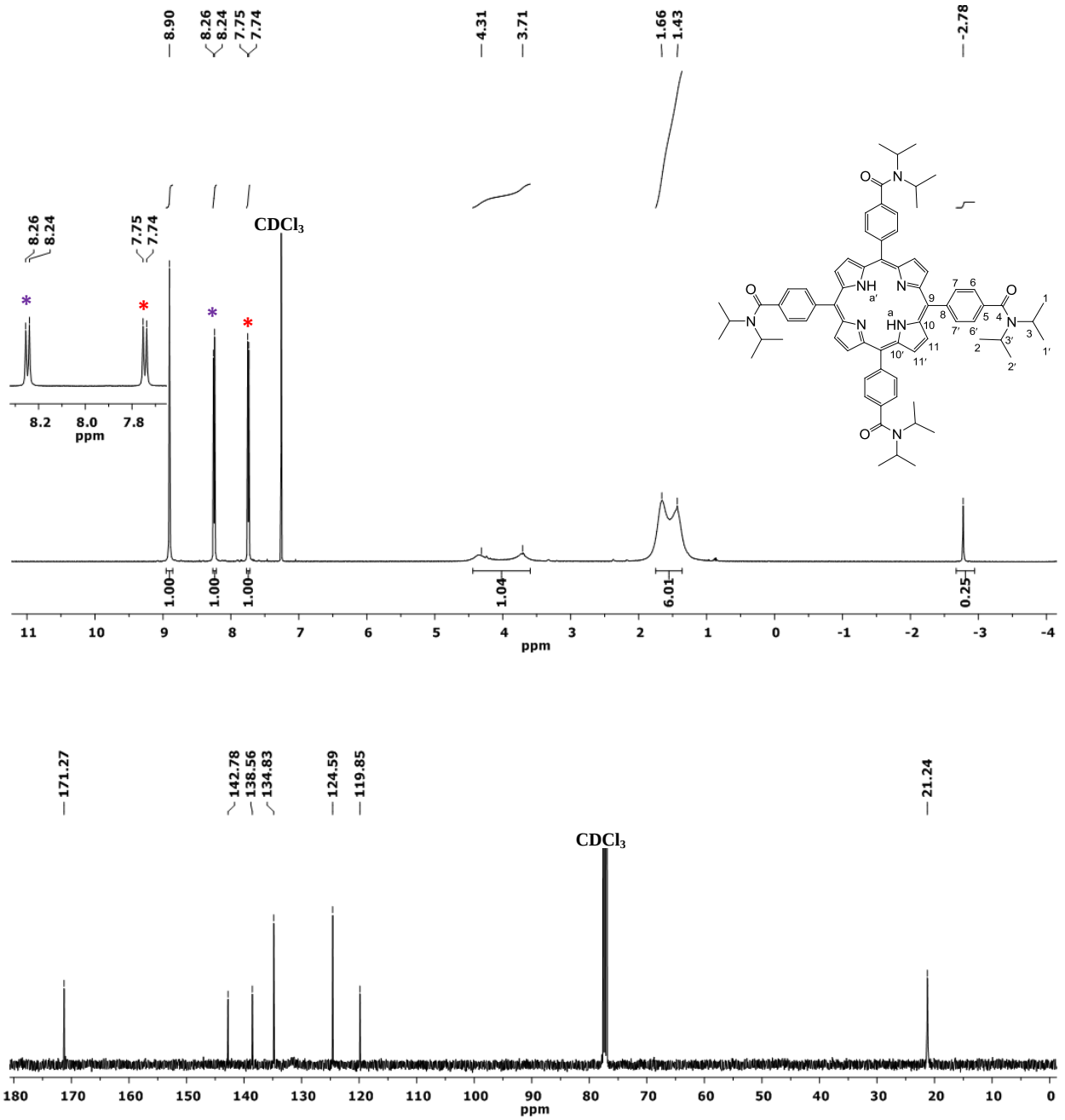

Figure S19: ^{1}H (above) and ^{13}C{^{1}H} NMR spectra (below) of **3**.

The ^{1}H NMR resonances of the N^{i}Pr$_2$ groups are all broadened. The hydrogen atoms H$^{1,1',2,2'}$ are regarded to correspond to the two broad singlets at 1.39 and 1.69 ppm. The hydrogen atoms H$^{3,3'}$ are regarded to correspond to the two singlets at 3.71 and 4.31 ppm. Both assignments could be, however, not verified by additional 2D NMR experiments (^{1}H,^{1}H-COSY,^{1}H,^{13}C-HSQCETGP and HMBCGP) which is attributed to too broad NMR resonances and/or to the comparatively poor solubility.

According to Jones and Wilkins [S1] for the -NMe$_2$ groups two ^{13}C NMR chemical shifts are observed. According to Manke et al. [S2] the ^{13}C NMR resonances of the pyrrole carbon atoms C$^{9,9'}$ and C$^{10,10'}$ are not observable.

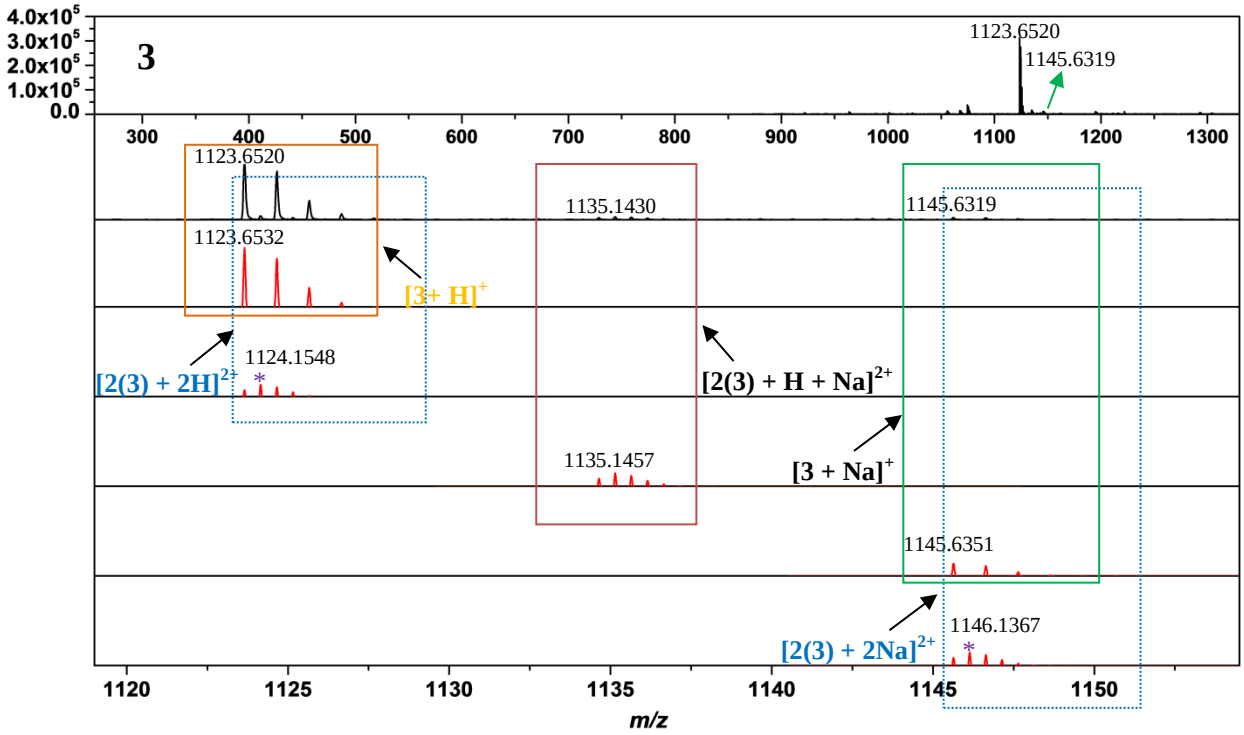

Figure S20: ESI-MS spectrum of **3** (Black: Measured. Red: Calculated).

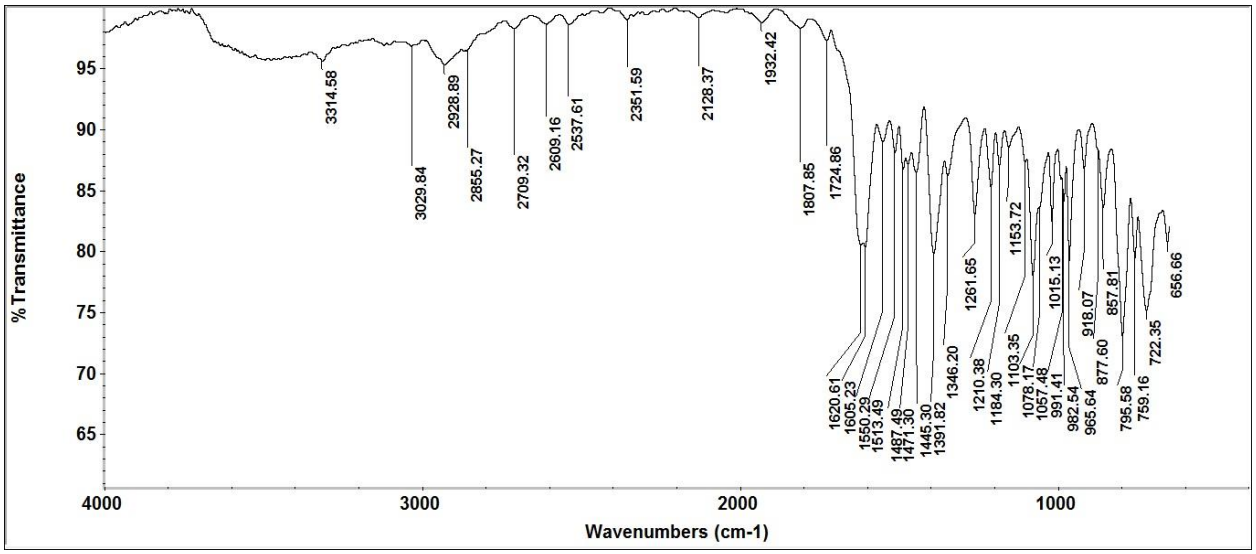

Figure S21a: IR spectrum (ATR-IR) of **3**.

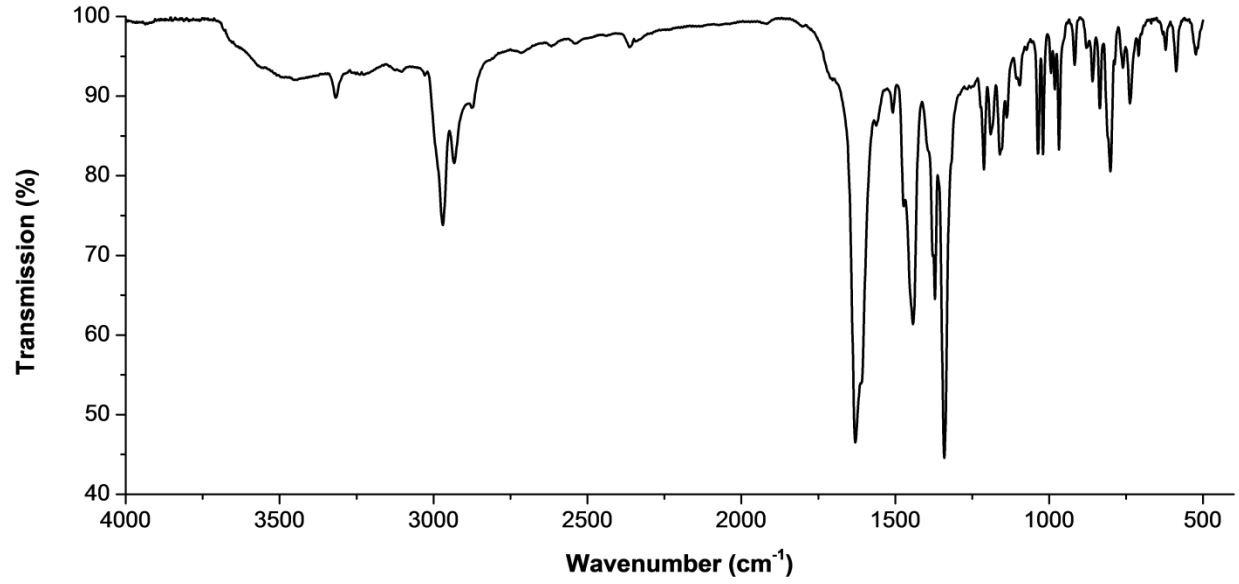

Figure S21b: IR spectrum (KBr) of **3**.

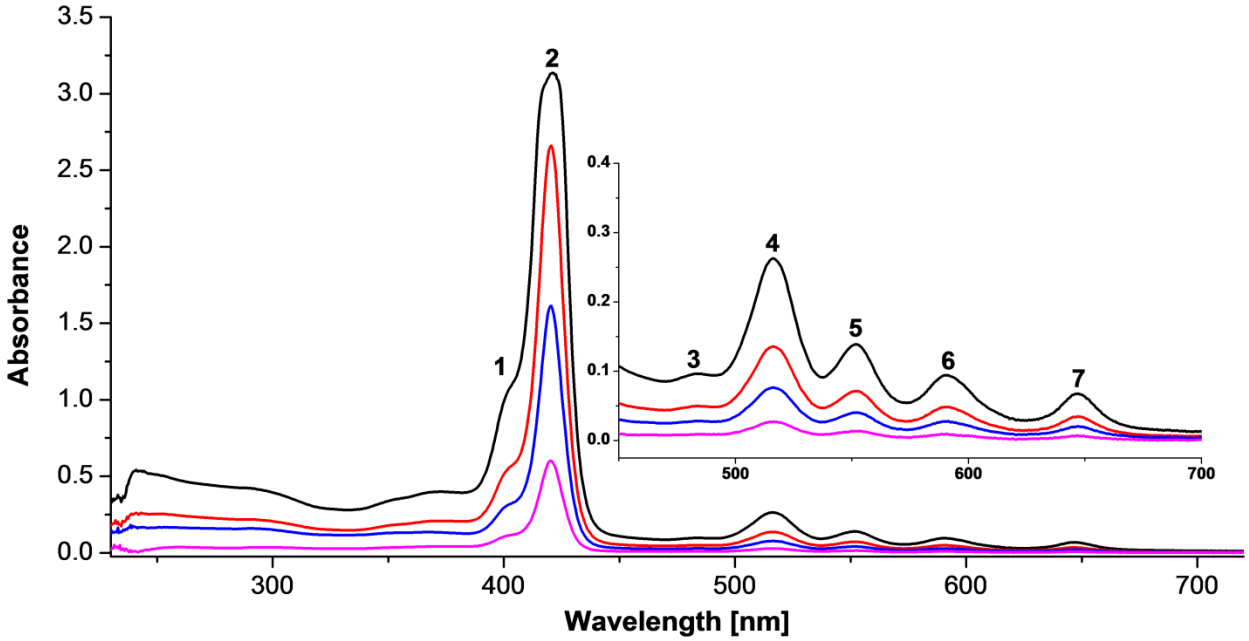

Figure S22: UV–vis spectrum of **3** in $CHCl_3$ at different concentrations.

Table S6: UV–vis data (λ_{max} [nm] log (ε [L·mol^{-1}·cm^{-1}])) of **3** at different concentrations.

	Absorption λ_{max} [nm] log (ε [L·mol^{-1}·cm^{-1}])						
	1	**2**	**3**	**4**	**5**	**6**	**7**
C_1 = 1.736·10^{-5} mol/L	399.1 (4.77)	421.1 (5.26)	481.7 (3.75)	516.5 (4.18)	551.2 (3.91)	590.7 (3.74)	647.3 (3.60)
C_2 = 1.157·10^{-5} mol/L	399.9 (4.66)	420.8 (5.36)	481.8 (3.65)	516.6 (4.07)	552.1 (3.80)	590.4 (3.65)	647.3 (3.51)
C_3 = 5.207·10^{-6} mol/L	400.1 (4.80)	420.2 (5.49)	481.7 (3.74)	516.5 (4.17)	552.1 (3.91)	591.2 (3.74)	647.8 (3.58)
C_4 = 1.736·10^{-6} mol/L	400.5 (4.86)	420.2 (5.54)	481.8 (3.70)	516.5 (4.20)	552.9 (3.97)	591.1 (3.75)	647.9 (3.67)

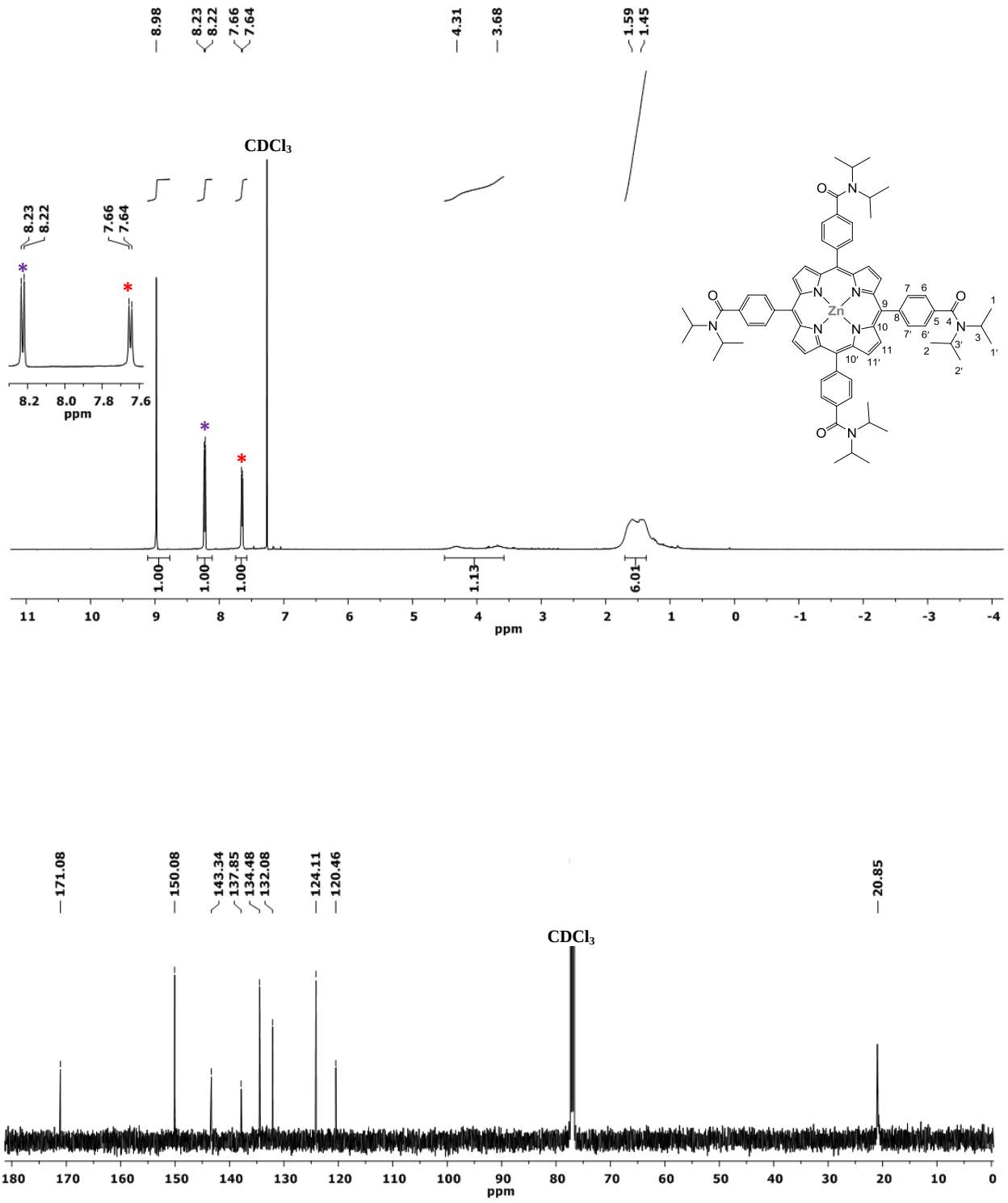

Figure S23: ^{1}H (above) and $^{13}C\{^{1}H\}$ NMR spectra (below) of **3a** in $CDCl_3$.

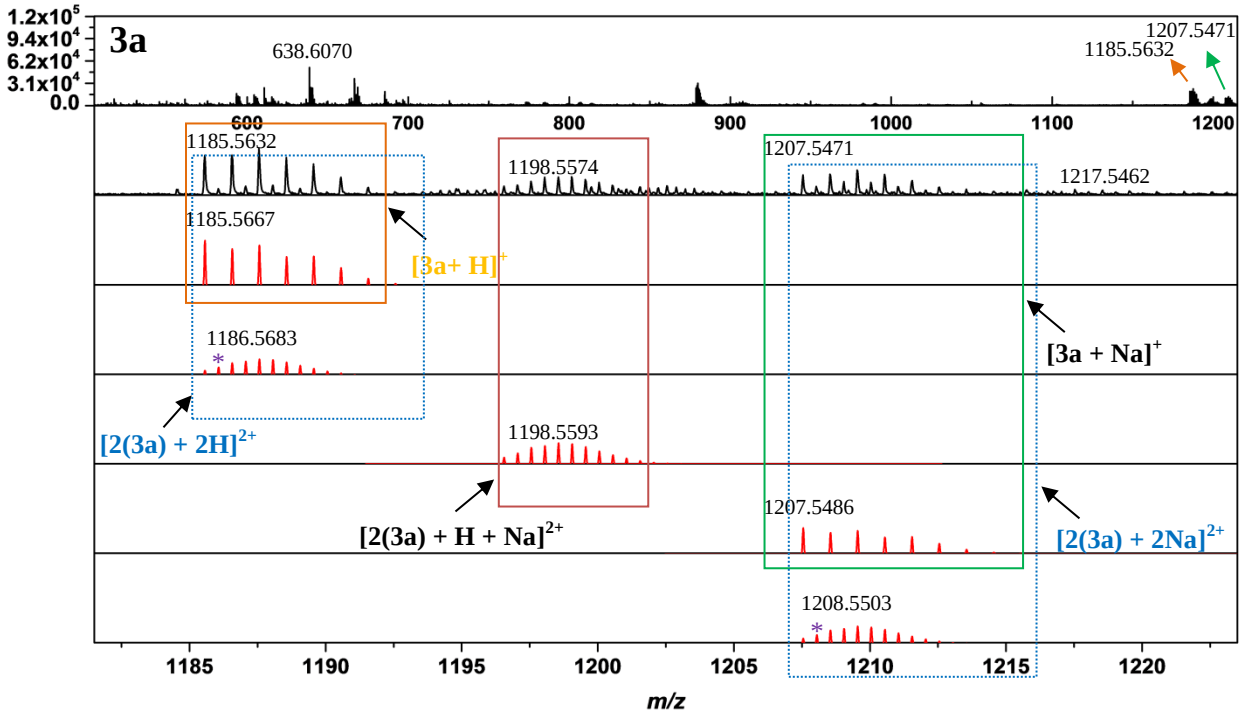

Figure S24: ESI-MS spectrum of **3a** (Black: Measured. Red: Calculated).

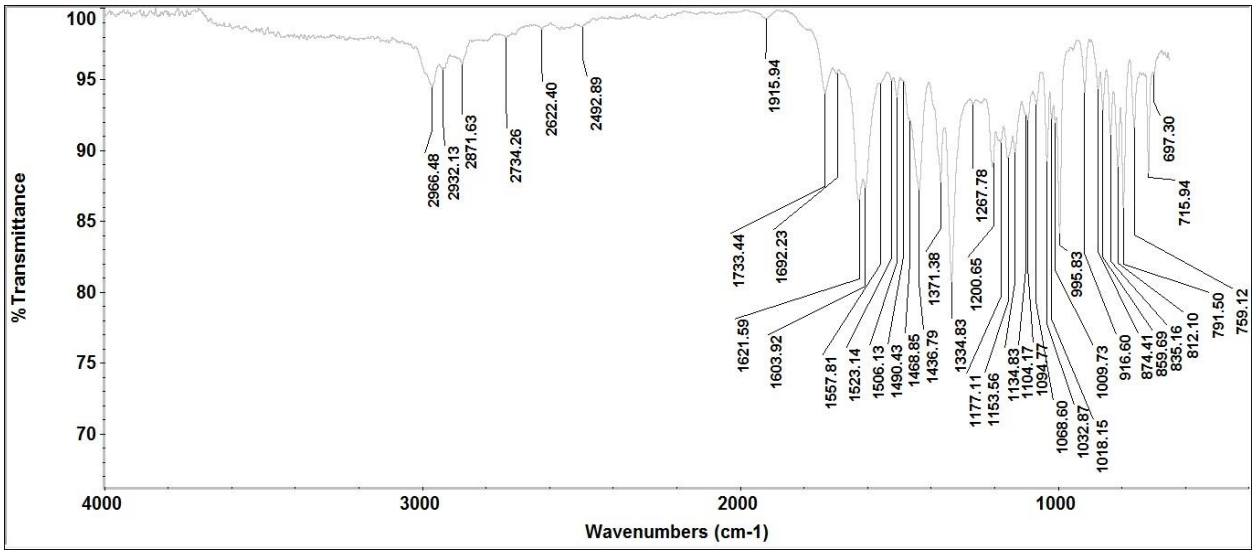

Figure S25a: IR spectrum (ATR-IR) of **3a**.

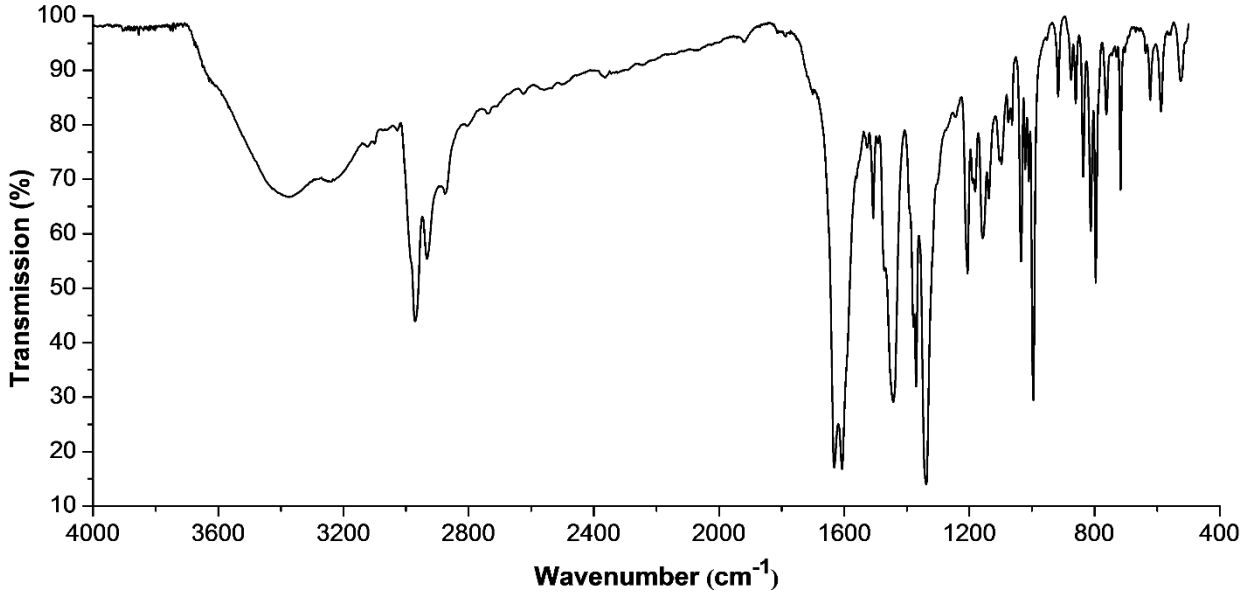

Figure S25b: IR spectrum (KBr) of **3a**.

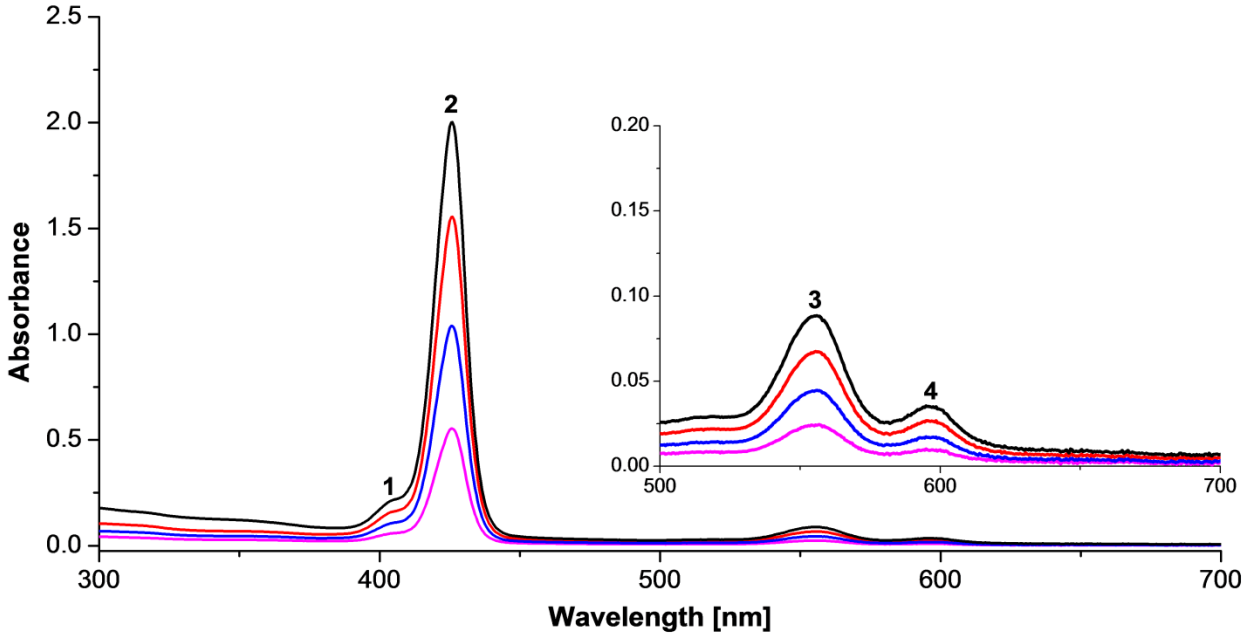

Figure S26: UV–vis spectrum of **3a** in $CHCl_3$ at different concentrations.

Table S7: UV–vis data (λ_{max} [nm] log (ε [$L \cdot mol^{-1} \cdot cm^{-1}$])) of **3a** at different concentrations.

	Absorption λ_{max} [nm] log (ε [$L \cdot mol^{-1} \cdot cm^{-1}$])			
	1	**2**	**3**	**4**
C_1 = 9.504·10^{-6} mol/L	404.3 (4.36)	425.9 (5.32)	555.8 (3.97)	596.7 (3.57)
C_2 = 7.920·10^{-6} mol/L	404.3 (4.33)	425.9 (5.29)	555.8 (3.93)	596.7 (3.53)
C_3 = 6.336·10^{-6} mol/L	403.6 (4.26)	425.9 (5.22)	555.8 (3.85)	596.7 (3.45)
C_4 = 1.584·10^{-6} mol/L	403.6 (4.57)	425.9 (5.55)	555.8 (4.19)	596.7 (3.78)

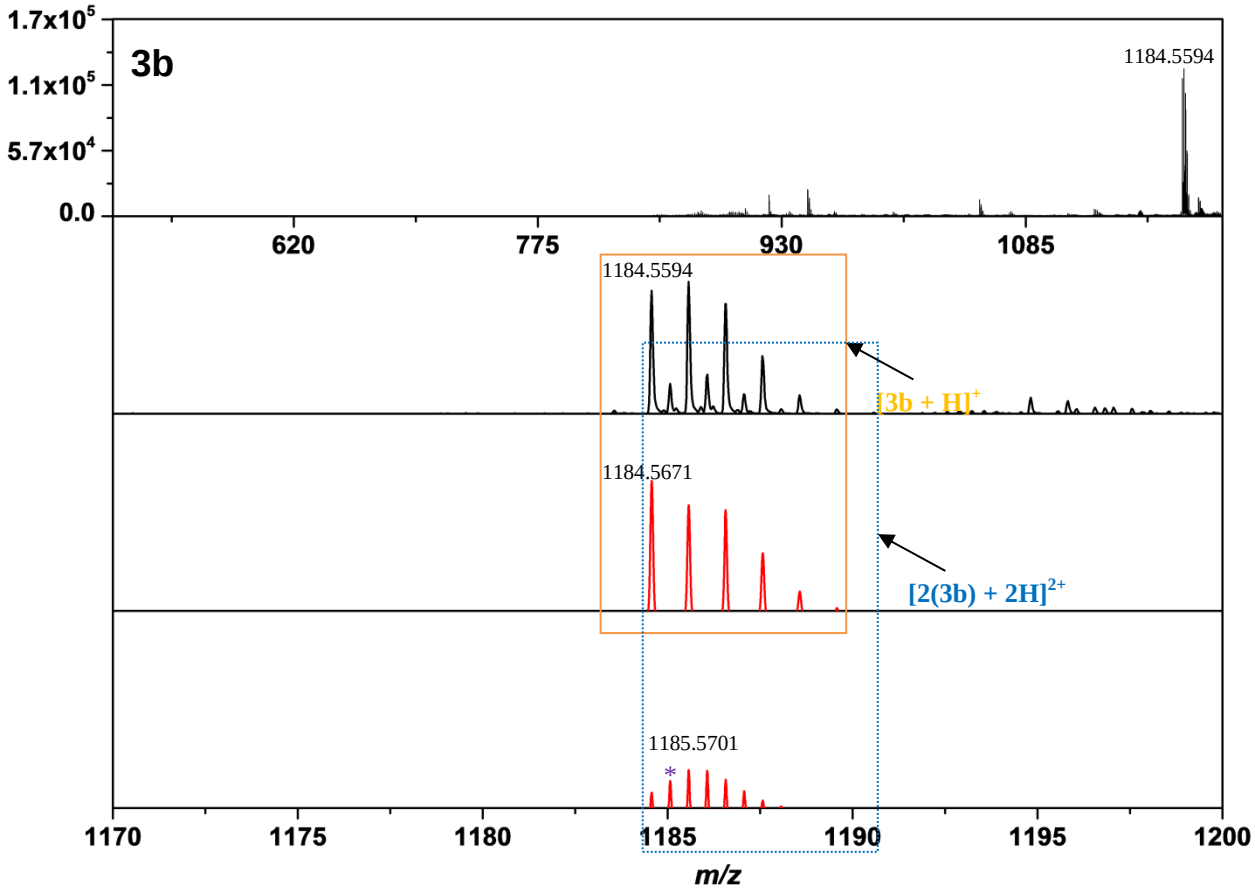

Figure S27: ESI-MS spectrum of **3b**. (Black: Measured. Red: Calculated).

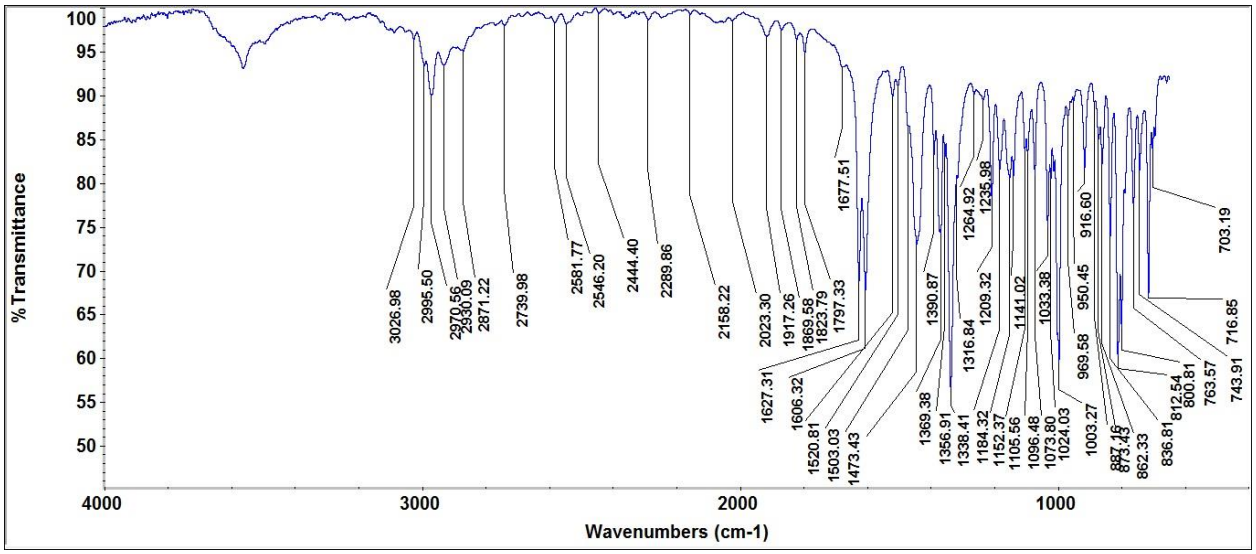

Figure S28a: IR spectrum (ATR-IR) of **3b**.

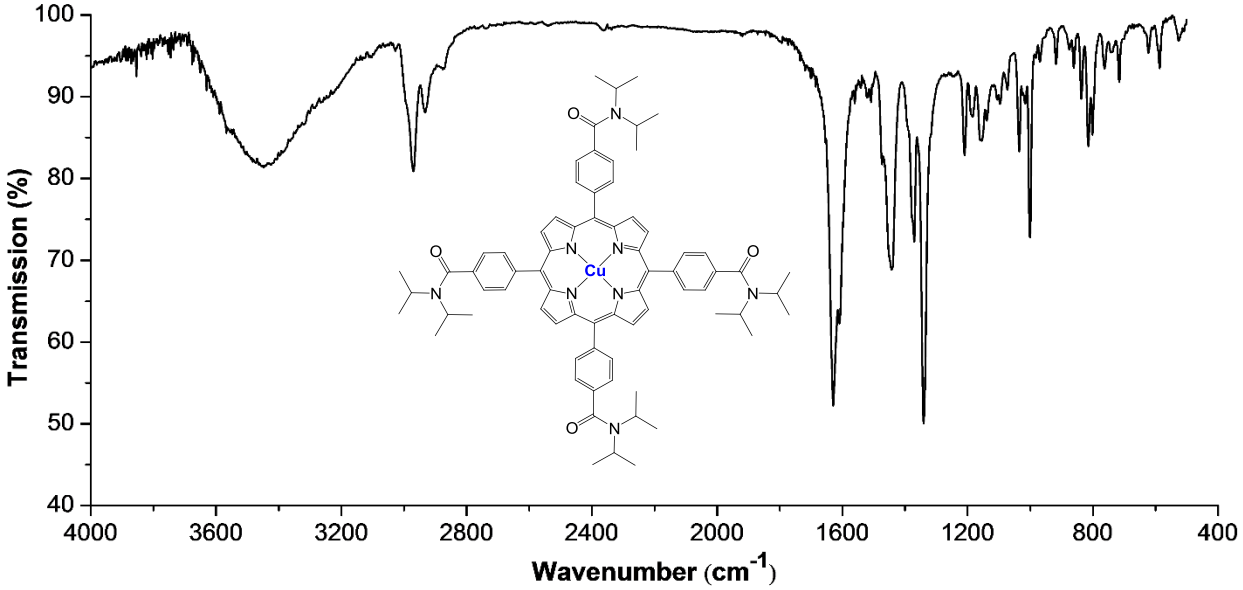

Figure S28b: IR spectrum (KBr) of **3b**.

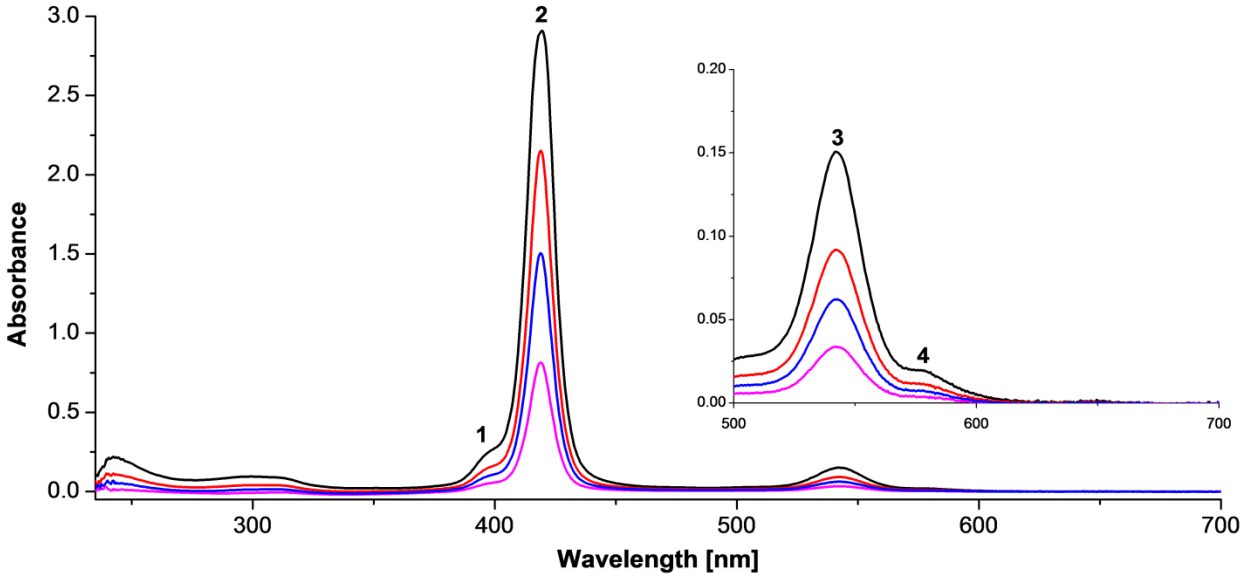

Figure S29: UV–vis spectrum of **3b** in $CHCl_3$ at different concentrations.

Table S8: UV–vis data (λ_{max} [nm] log (ε [L·mol^{-1}·cm^{-1}])) of **3b** at different concentrations.

	Absorption λ_{max} [nm] log (ε [L·mol^{-1}·cm^{-1}])			
	1	**2**	**3**	**4**
C_1 = 5.401·10^{-6} mol/L	397.3 (4.61)	419 (5.69)	542.4 (4.36)	579.1 (3.44)
C_2 = 4.051·10^{-6} mol/L	397.3 (4.58)	419 (5.72)	542.4 (4.36)	579.1 (3.46)
C_3 = 2.700·10^{-6} mol/L	397.3 (4.58)	419 (5.74)	542.4 (4.37)	579.1 (3.43)
C_4 = 1.350·10^{-6} mol/L	397.3 (4.58)	419 (5.78)	542.4 (4.39)	579.8 (3.46)

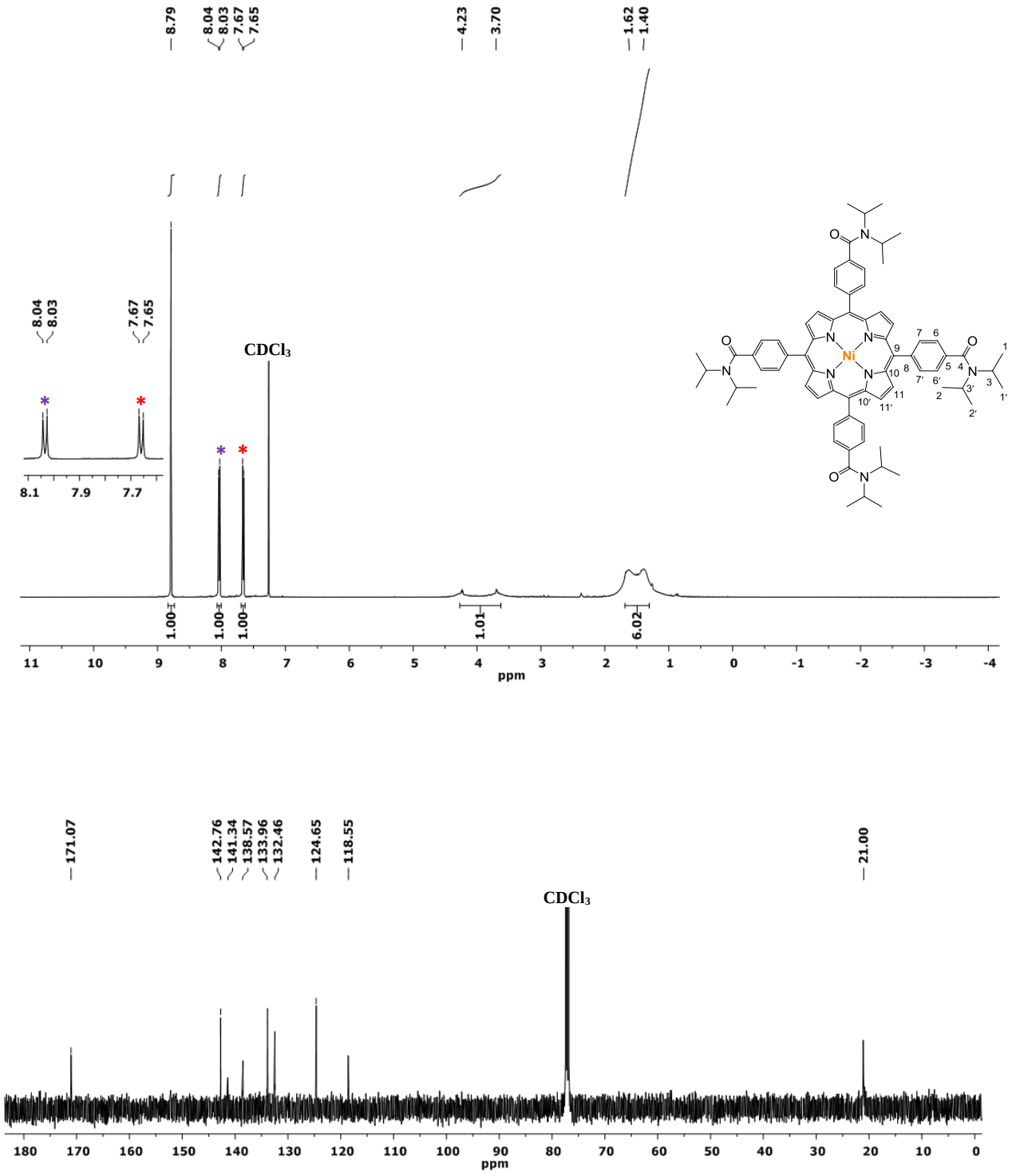

Figure S30: ^{1}H (above) and $^{13}C\{^{1}H\}$ NMR spectra (below) of **3c**.

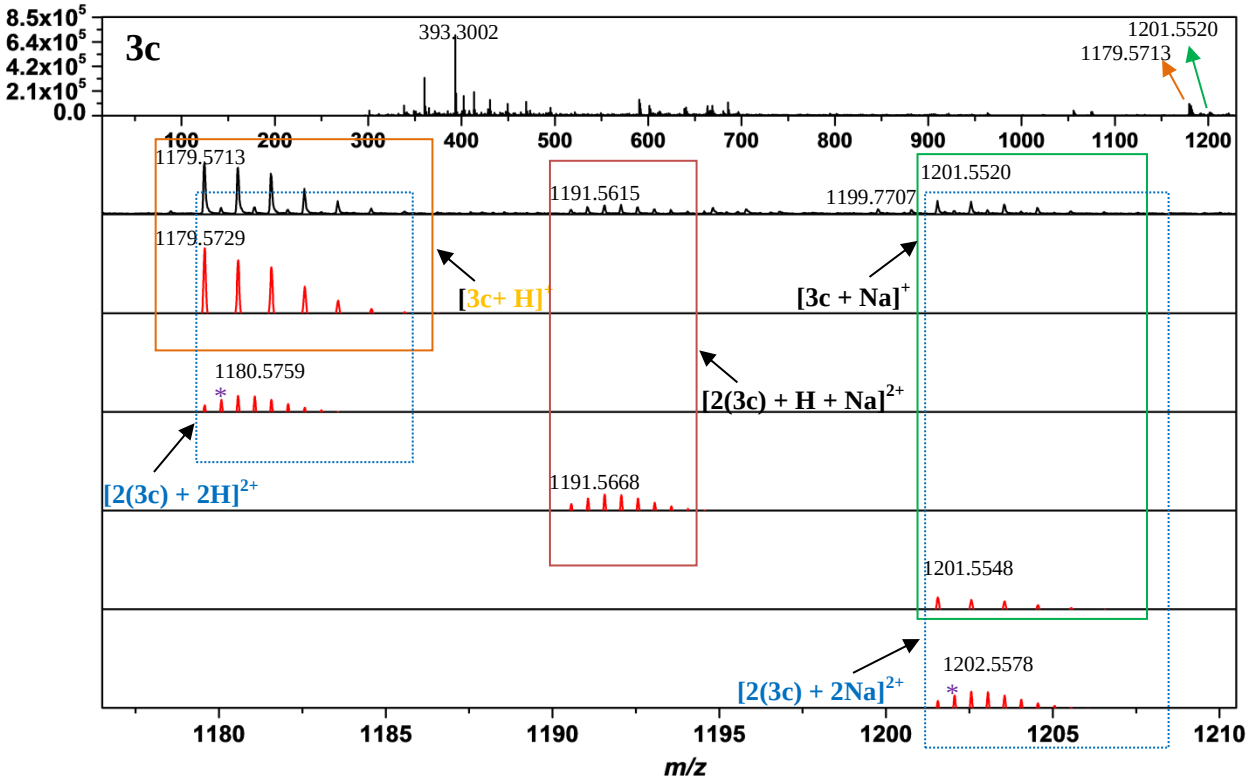

Figure S31: ESI-MS spectrum of **3c** (Black: Measured. Red: Calculated).

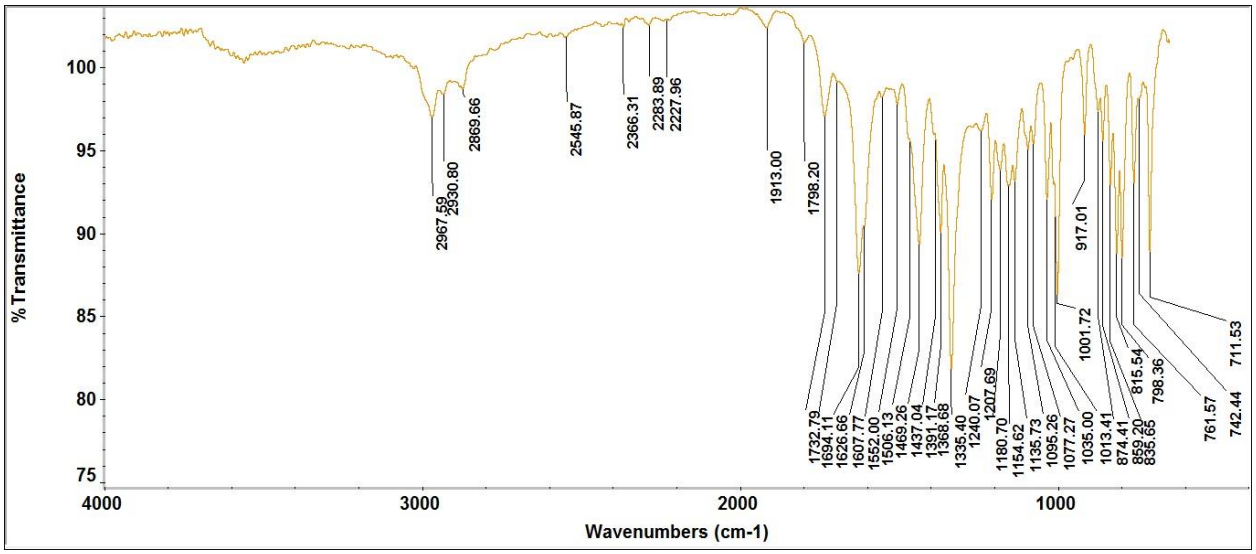

Figure S32a: IR spectrum (ATR-IR) of **3c**.

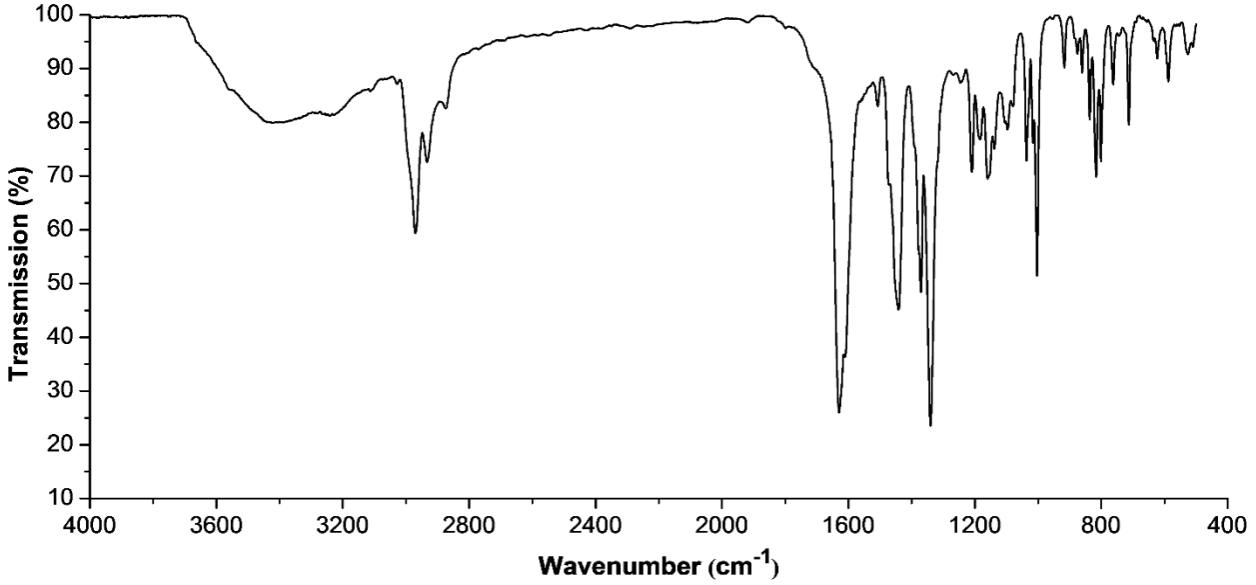

Figure S32b: IR spectrum (KBr) of **3c**.

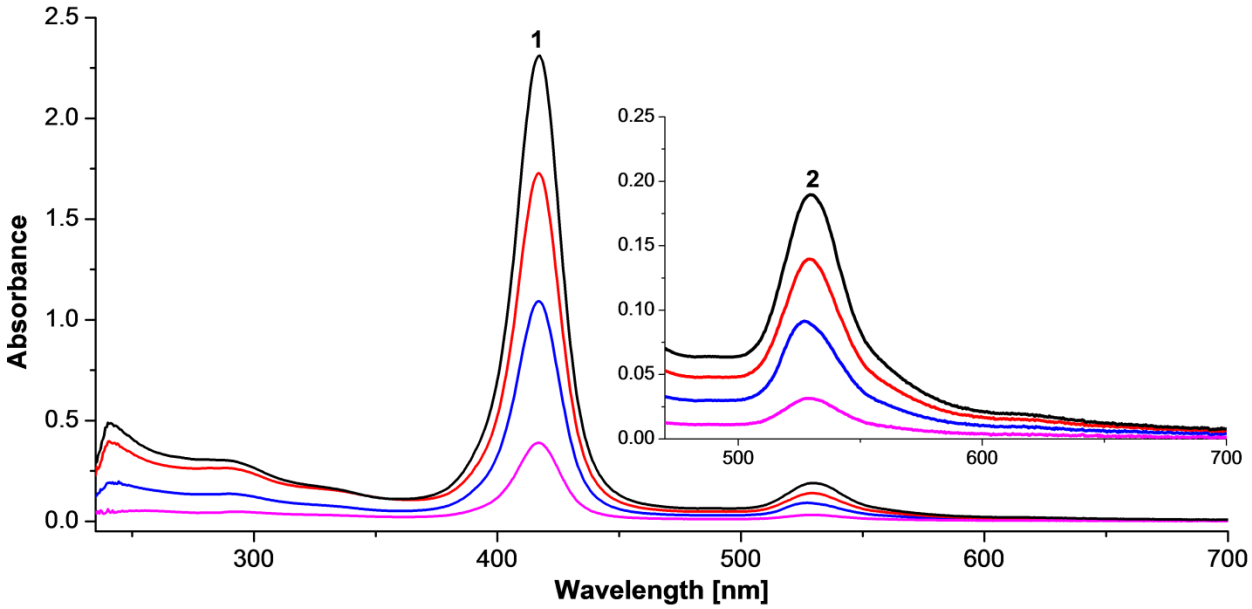

Figure S33: UV–vis spectrum of **3c** in $CHCl_3$ at different concentrations.

Table S9: UV–vis data (λ_{max} [nm] log (ε [L·mol^{-1}·cm^{-1}])) of **3c** at different concentrations.

	Absorption λ_{max} [nm] log (ε [L·mol^{-1}·cm^{-1}])	
	1	**2**
C_1 = **1.151·10^{-5} mol/L**	417.2 (5.30)	529.8 (4.22)
C_2 = **8.219·10^{-6} mol/L**	417.2 (5.32)	529.5 (4.23)
C_3 = **4.932·10^{-6} mol/L**	417.2 (5.35)	527.2 (4.27)
C_4 = **1.644·10^{-6} mol/L**	417.2 (5.38)	529.5 (4.29)

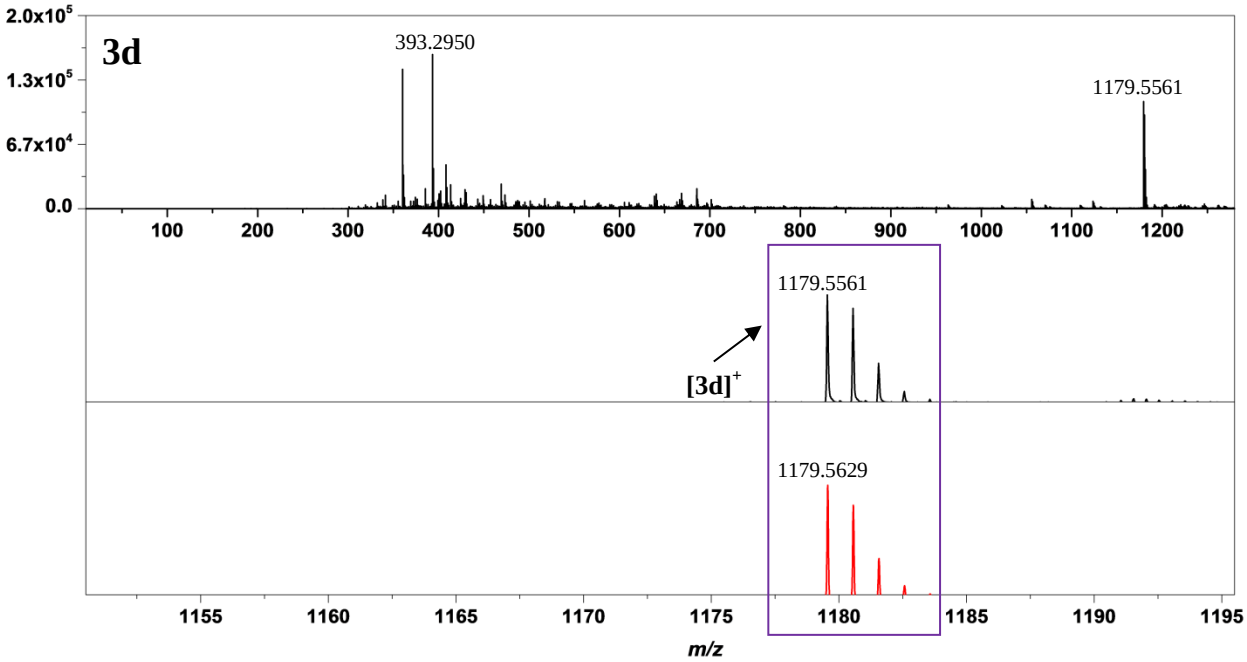

Figure S34: ESI-MS spectrum of **3d** (Black: Measured. Red: Calculated).

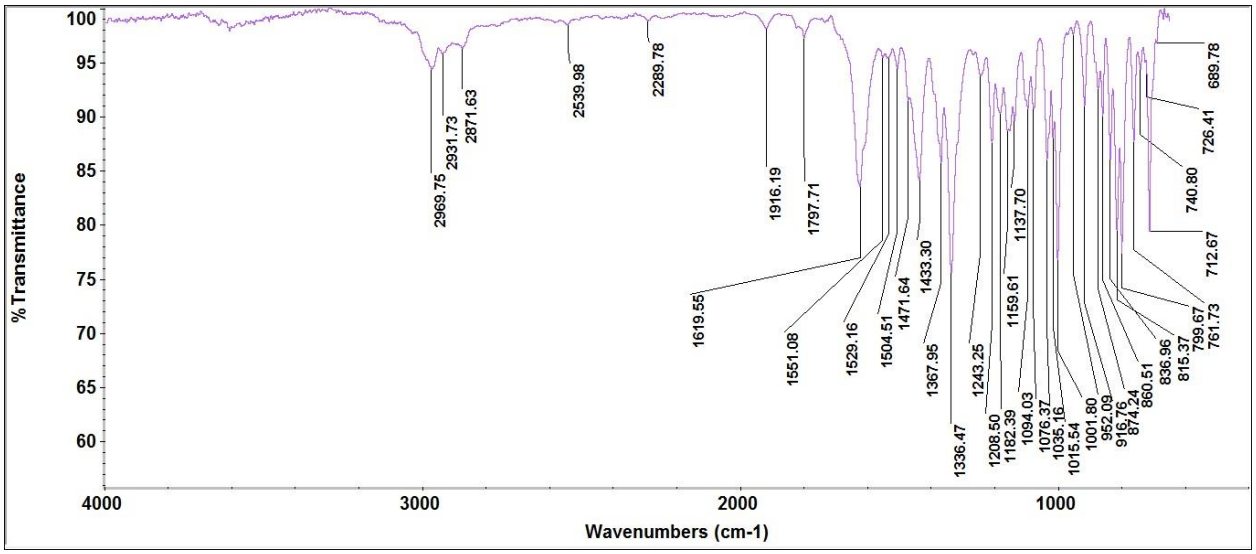

Figure S35a: IR spectrum (ATR-IR) of **3d**.

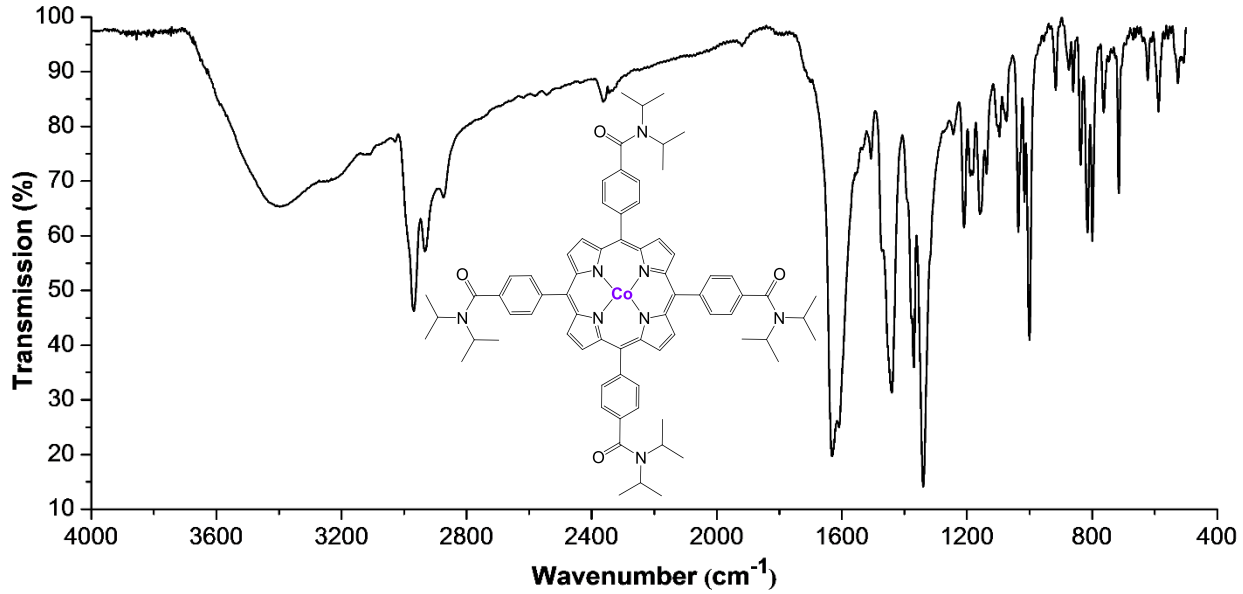

Figure S35b: IR spectrum (KBr) of **3d**.

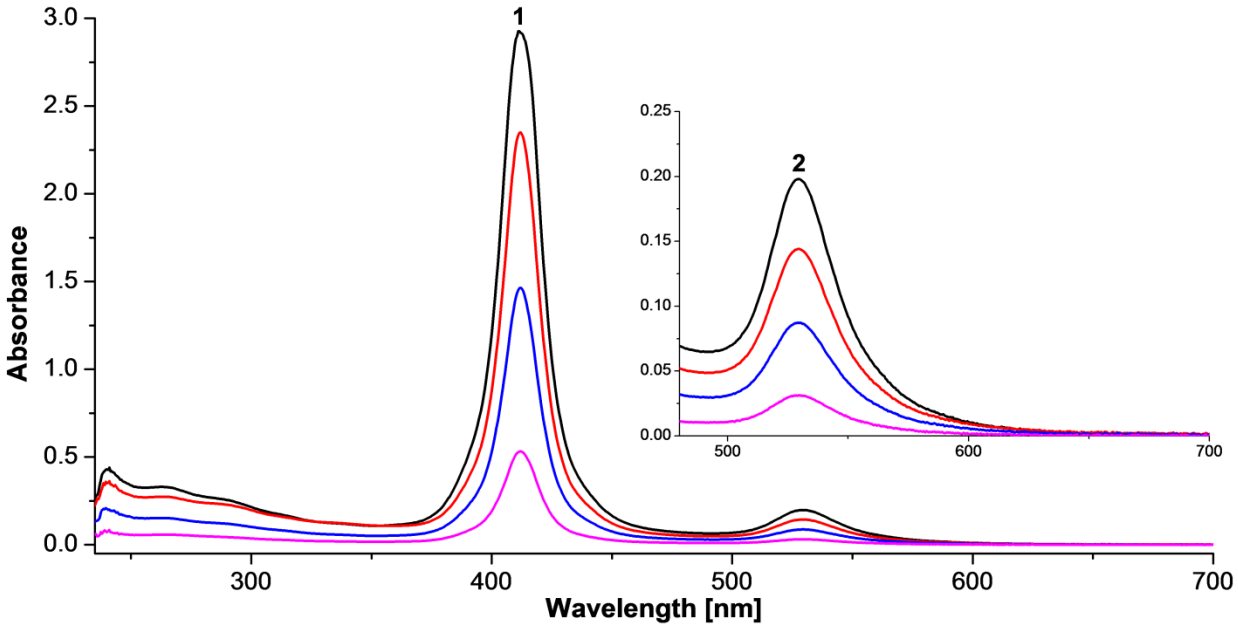

Figure S36: UV–vis spectrum of **3d** in $CHCl_3$ at different concentrations.

Table S10: UV–vis data (λ_{max} [nm] log (ε [$L \cdot mol^{-1} \cdot cm^{-1}$])) of **3d** at different concentrations.

	Absorption λ_{max} [nm] log (ε [$L \cdot mol^{-1} \cdot cm^{-1}$])	
	1	**2**
C_1 = 1.148·10^{-5} mol/L	412.3 (5.41)	529.4 (4.10)
C_2 = 8.203·10^{-6} mol/L	412.3 (5.45)	529.4 (4.24)
C_3 = 4.922·10^{-6} mol/L	412.3 (5.47)	529.4 (4.25)
C_4 = 1.641·10^{-6} mol/L	412.3 (5.51)	529.4 (4.28)

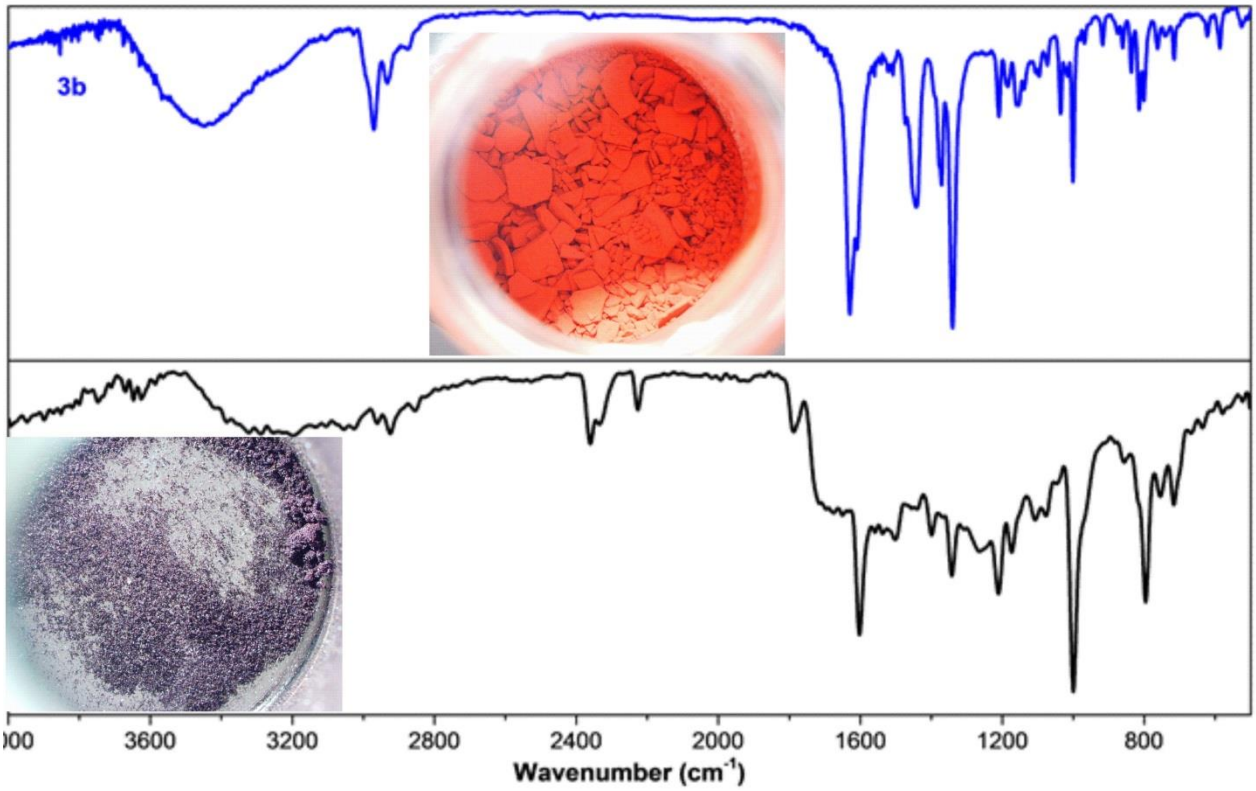

Figure S37: IR spectra (KBr) of **3b** (above) and in comparison to remains of **3b** after OMBD trials (below). Optical photographs of the material before (red) and after (purple) OMBD.

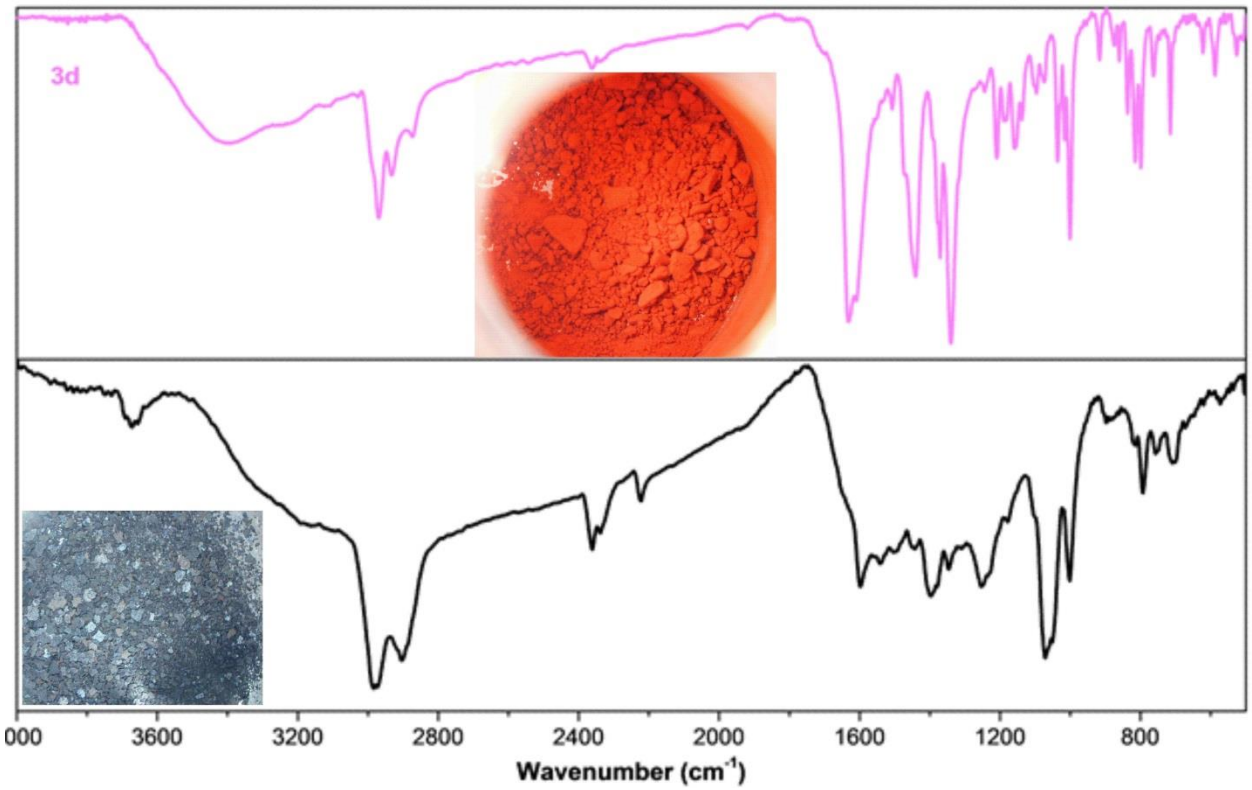

Figure S38: IR spectra (KBr) of **3d** (above) and in comparison to remains of **3d** after OMBD trials (below).

Optical photographs of the material before (red) and after (purple) OMBD.

References

S1 Jones, R. G.; Wilkins, J. M. *Organic Magnetic Resonance*. **1978**, *11*, 20–26. doi:10.1002/mrc.1270110102

S2 Manke, A. M.; Geisel K.; Fetzer, A.; Kurz, P. *Phys. Chem. Chem. Phys*. **2014**, *16*, 12029–12042. doi:10.1039/c3cp55023k